

1970

Laboratory investigation into evaluation of aperture-to-medium coupling loss

Duane Foster Rost
Iowa State University

Follow this and additional works at: <https://lib.dr.iastate.edu/rtd>

 Part of the [Electrical and Electronics Commons](#)

Recommended Citation

Rost, Duane Foster, "Laboratory investigation into evaluation of aperture-to-medium coupling loss " (1970). *Retrospective Theses and Dissertations*. 4787.

<https://lib.dr.iastate.edu/rtd/4787>

This Dissertation is brought to you for free and open access by the Iowa State University Capstones, Theses and Dissertations at Iowa State University Digital Repository. It has been accepted for inclusion in Retrospective Theses and Dissertations by an authorized administrator of Iowa State University Digital Repository. For more information, please contact digirep@iastate.edu.

71-7320

ROST, Duane Foster, 1940-
LABORATORY INVESTIGATION INTO EVALUATION OF
APERTURE-TO-MEDIUM COUPLING LOSS.

Iowa State University, Ph.D., 1970
Engineering, electrical

University Microfilms, Inc., Ann Arbor, Michigan

**LABORATORY INVESTIGATION INTO EVALUATION OF
APERTURE-TO-MEDIUM COUPLING LOSS**

by

Duane Foster Rost

**A Dissertation Submitted to the
Graduate Faculty in Partial Fulfillment of
The Requirements for the Degree of
DOCTOR OF PHILOSOPHY**

Major Subject: Electrical Engineering

Approved:

Signature was redacted for privacy.

In Charge of Major Work

Signature was redacted for privacy.

Head of Major Department

Signature was redacted for privacy.

Dean of Graduate College

**Iowa State University
Ames, Iowa**

1970

TABLE OF CONTENTS

	Page
INTRODUCTION	1
REVIEW OF LITERATURE	5
EXPERIMENTAL DESIGN	21
Transmitter	21
Propagation Path	21
Receiver	25
Recording System	25
EXPERIMENTAL RESULTS	39
SUMMARY	59
LITERATURE CITED	61
ACKNOWLEDGEMENTS	65

INTRODUCTION

The work described can be broken into two separate areas. The first is the development and validation of a practical technique to experimentally evaluate aperture-to-medium coupling loss. The second is the use of the technique to measure the effect of aperture-to-medium coupling loss over a wide range of aperture sizes for a particular propagation path.

The experimental apparatus consisted of a high frequency source of high power density, monochromatic, coherent energy, a transmitting aperture, a propagation path, and various receiving apertures coupled to a recording system. The use of a helium-neon laser resulted in a size reduction of more than one million to one in comparing a typical tropospheric scatter link to the laboratory setup. Though the comparison was limited regarding the precise shape of the propagation path, the capability of the model was such as to make it a valuable tool for radio wave propagation research.

The concepts of directive gain and aperture-to-medium coupling loss must be clearly understood before the discussion of theoretical or experimental investigations will have any meaning. It is essential to define terms carefully and to tie the somewhat abstract mathematical statements to an "intuitive feeling" for the concept. Without that "feeling" it is easy to become lost in the supporting issues and not completely grasp the significance of the results or the applications of them.

The gain function is most easily evaluated in spherical coordinates

as it is a function of the direction of radiation and not the range (1). The gain function $g(\theta, \phi)$ is the ratio of the power radiated in the direction (θ, ϕ) per unit solid angle ($\hat{p}(\theta, \phi)$) to the average power radiated per unit solid angle ($p/4\pi$ where p is the total radiated power).

$$g(\theta, \phi) = \frac{4\pi\hat{p}(\theta, \phi)}{p} \quad (1)$$

The gain function of an isotropic radiator is unity as is seen from the definition of isotropic (equal in all directions). The free-space gain of any antenna above an isotropic radiator is expressed in decibels (dB) as

$$G = 10 \log_{10} g_{\max}(\theta, \phi) \quad (2)$$

Norton (2,3) described the recommendations of the Consultative Committee on International Radio (CCIR) on standardization of terminology to be used in radio wave propagation. The basic transmission loss (L_b) is the loss expected between an ideal, loss-free, isotropic transmitter and receiver at the same locations as the actual transmitter and receiver and influenced by the same propagation path. It is the ratio p_{it}/p_{ir} , where p_{it} is the total power from an isotropic transmitter and p_{ir} is the total power received by an isotropic receiver.

$$L_b(\text{dB}) = 10 \log_{10} \frac{p_{it}}{p_{ir}} \quad (3)$$

The transmission loss (L) of a link consisting of a transmitter, a receiver, and the intervening propagation medium is the ratio p_t/p_r , where p_t is the total radiated power and p_r is the total received power.

$$L(\text{dB}) = 10 \log_{10} \frac{p_t}{p_r} \quad (4)$$

The distinction between L_b and L is L accounts for the actual

antennas. The difference is the path-antenna directivity gain (G_p).

$$G_p = L_b - L \quad (5)$$

A word statement of G_p may be quoted from Norton as, "The path-antenna directivity gain is equal to the increase in the transmission loss when lossless, isotropic antennae are used at the same locations as the actual antennae." In specialized cases G_p may equal the sum of the free-space gains of the transmitter and receiver. It is also possible for G_p to be negative for cases such as a vertically-polarized transmitter and a horizontally polarized receiver. However in most cases G_p will be positive and closely related to the sum of the antenna gains.

$$G_p = G_t + G_r - L_c \quad (6)$$

where L_c is the loss in antenna gain in dB and is commonly called the aperture-to-medium coupling loss. Several authors have considered this loss to be part of the basic transmission loss. Intuitively aperture-to-medium coupling loss is the failure of a system to realize the calculated free-space gains of the antennas used. A discussion of the past theoretical and experimental investigations is presented in the next section, but one point must be made clear before considering the details of each study. The experimental work can only evaluate a relative or incremental aperture-to-medium coupling loss between any two test combinations. This is shown by assuming the basic transmission loss term does not change, substituting into Equation 6 and subtracting for two different receiving apertures.

$$\Delta G_p = G_{p2} - G_{p1} = G_{t2} - G_{t1} + G_{r2} - G_{r1} - (L_{c2} - L_{c1}) \quad (7)$$

The measurements yield ΔG_p . With $G_{t2} = G_{t1}$, and $\Delta G_r = G_{r2} - G_{r1}$, available from free-space measurements or calculations (if direct measurement of G_r is not possible),

$$\Delta L_c = L_{c2} - L_{c1} = \Delta G_r - \Delta G_p \quad (8)$$

Thus only an incremental aperture-to-medium coupling loss is observable from normal experiments changing one or more antenna sizes. Only Hartman (4) and Gough (5) among the authors cited discuss this limitation.

Friis, et al. (6) show, without comment, power ratio changes resulting from changing only one antenna.

Staras (7) concurred with part of Hartman's discussion on limitations of coupling loss information available from measurements, but restricted his comments to saying both antennas must be considered, not just one.

REVIEW OF LITERATURE

Investigations of extended-range or transhorizon tropospheric transmission date back at least thirty five years to when Marconi received 400 MHz signals over a distance of about 250 km in the Mediterranean south of France (8). In the intervening years many theories have been proposed to explain the observed field intensities in the region below the radio horizon. These field intensities are significantly stronger than predicted by the application of diffraction theory to a smooth airless earth. DuCastel (9) presented a good background coverage of tropospheric radio wave propagation with an exceptionally complete bibliography through 1963. A short resume of the major theories will aid in placing the study of aperture-to-medium coupling loss in proper perspective.

The turbulent scattering theory of radio wave propagation has been given the most attention and widest acceptance at this time. This theory states that the scattering of radio waves is caused by turbulence-induced departures from the mean refractive index (1,10-15). Direct measurements of the meteorological conditions (16) indicated the scale of the turbulence may vary from a few centimeters to several kilometers. The measured gradient of the refractive index was limited by the recorder response. Quoting from the JTAC (17), "After careful normalization of such factors a frequency, antenna aperture-to-medium coupling loss, surface refractive index, atmospheric gaseous absorption, path height, surface distance, and angular distance, good agreement can be obtained between observed and calculated median transmission loss out to distances of some 600 statute miles, when the assumption is made the intensity of

the turbulence decreases exponentially with height. Here, good agreement is defined as a 6 dB RMS deviation of the long-term medium winter fields from prediction." Airborne refractive index measurements demonstrated a distinct stratification was present at least half the time in many locations (12). Rapid beam-swinging experiments (18) have shown partial reflecting layers and observed movement and rapid changes in the atmosphere structure such as might have been caused by a ripple motion propagating at velocities of from 1000 to 1300 km/h. Additional study of tropospheric structure by high resolution antennas (19) has observed as many as four reflecting layers in one vertical sweep. No clear transition exists from the turbulent layer scattering to layer reflection theories (6). However the reflection theory discusses sharper gradients in the refractive index as a function of height. The normal mode theory assumes the gradual decrease in the refractive index with height causes a small fraction of the radio wave energy to be coherently reflected downward from all heights. The assumptions made concerning the exact form of the gradient attempt to agree with the physical measurements, yet allow mathematical solution of the resulting equations. Bullington (15) sums up the discussion of tropospheric propagation theories, "If the problem of inhomogeneous atmosphere could be solved rigorously, there would be no difference of opinion, but a rigorous solution that can be readily evaluated has not yet been achieved without significant approximations, and the relative accuracy of the different approximations is in question." Of course the lack of a complete and accepted description of the atmosphere has not hastened the resolution of tropospheric propagation questions.

It is against this diverse background of tropospheric work that the

question of aperture-to-medium must be considered. Figure 1 is an idealized sketch of the common volume "seen" by both the transmitter and the receiver. The dimensions and the medium included in the common volume are of prime interest in the theories dealing with loss analysis. Booker and deBettencourt seem to have coined the term "aperture-to-medium coupling loss" in 1955 (11). They developed their theory on the hypothesis that antenna beams narrower than a critical angle α_c ($\alpha_c = (2/3)(d/a)$, where d was the range between antennas and a the earth's radius modified for normal atmospheric refraction) would not effectively encompass all the atmosphere capable of contributing to the scattered power at the receiver. They then stated, (replacing d/a by the scatter angle θ .)

$$L_c = 0.43 \left(\frac{\theta}{\alpha} \right)^3 \quad (9)$$

where α was the beamwidth of the equal transmitting and receiving antennas and $\alpha \ll \alpha_c$.

Staras (20) considered the atmosphere to be anisotropic and defined an anisotropy parameter as the ratio of the vertical scale of turbulence to the horizontal scale of turbulence. He removed the restriction of identical antennas at each end by defining an effective beamwidth (α_0) as

$$\alpha_0^{-2} = \alpha_t^{-2} + \alpha_r^{-2} \quad (10)$$

where α_t and α_r are the beamwidths of the transmitter and receiver respectively. Separate expressions for horizontal and vertical dimension losses in dB were developed and the total loss evaluated by summing them. The horizontal component was found to vary as $\theta/\alpha_{0\text{horizontal}}$ and the vertical as $(\theta/\alpha_{0\text{vertical}})^2$. Summation of the dB loss terms is

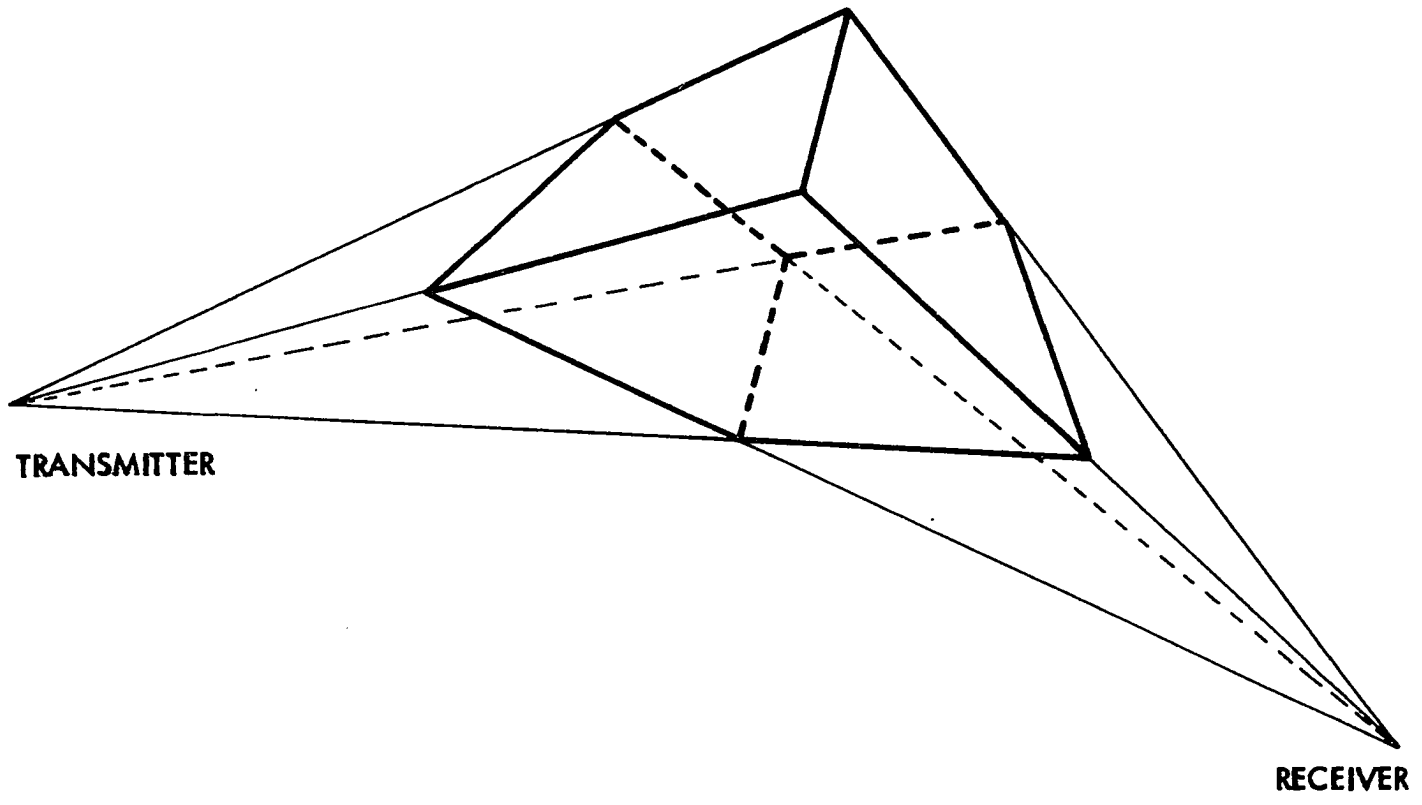


Figure 1. Idealized antenna patterns showing common volume

equivalent to multiplying the factors, so the total loss (L_c) was shown to vary as $\sigma^3 / \alpha_{0h} \alpha_{0v}^2$. Though quite similar to Booker and deBettencourt's result given as Equation 9, the vertical dimension played a dominant role. The increased effect of the vertical beamwidth comes from the assumption by Staras that the intensity of the turbulence decreased inversely as the square of the height while Booker and deBettencourt assumed the turbulence to be constant.

In 1958, Waterman (14) arrived at a quite similar form which he gave as

$$L_c = C_m \left(\frac{\sigma}{\alpha}\right)^r \quad (11)$$

where α was the geometric mean of the narrow beamwidths and r ranged from 1 to 3 depending on the horizontal and vertical beamwidths of both the transmitting and the receiving antennas. C_m values were determined by consideration again of the two beamwidths for each antenna. The scattering turbulence was assumed constant but an "effective volume" was employed which again gave privileged status to the vertical beamwidths. He included an extensive scheme for selecting the values for C_m , r , and α and stated, "An important point to note, however, is the number of adjustable parameters available for obtaining agreement with experiment."

In 1959 Hartman and Wilkerson (1) assumed an exponential decrease with height of the variance of the refractive index divided by the scale of turbulence. They arrived at a family of curves depending on the selected rate of decay of the variance of the refractive index with height that were basically similar in form to those of Booker-deBettencourt and Staras. A difference in the form of presentation made it necessary to select a reasonable set of values to allow comparison with the earlier

theories. The effect of the rate of decay of the variance was to lessen the rapid increase in loss with distance.

Friis, et al. (6) in their reflection theory for beyond the horizon propagation presented a power ratio created by changing the vertical beam widths of one antenna. They showed results for one case assuming the reflection coefficient varied as the inverse sixth power of height. Their only comment was that continued increases in the antenna dimensions results in less and less increase in received power.

Bullington (15) in 1963 approached the problem by evaluating meteorological data and noting the variance of the permittivity decreased with height at the same rate as the mean. As the reflection coefficient mean value was caused by the exponential decrease in the permittivity and the irregularities superimposed on the decrease in the permittivity caused the variance of the permittivity to vary as the mean, he assumed the variance of the reflection coefficient also varied as its mean. This assumption resulted in an antenna degradation term in the reflection coefficient of the form $(1 - e^{-\frac{b\alpha d}{2}})^{\frac{1}{2}}$ where b was the rate of decrease of permittivity, α the beamwidth and d the total distance. The trend of increasing loss with increasing size of the antennas (α decreasing) was in agreement with the other theories. However the conclusion that the amount of the loss decreased with distance was in sharp disagreement with earlier published analyses.

Armand and Vvedenskii (21) had, four years earlier, published a theory which arrived at almost identical results as Bullington's in regard to the inverse distance dependence. Their approach to the problem and their assumptions were entirely different from Bullington's. They

proposed that the angle-of-arrival of the power was the critical feature, and they worked out their results assuming an incident field which was constant (not a function of angle-of-arrival) in a cone from the antenna and zero elsewhere. This assumption ignored a better description by Gordon (12). There also seemed to be a mathematical error (7) that would significantly change the results. Consequently, extreme care must be used in applying their conclusions. However the differences in method between their work and Bullington's must be remembered and Bullington's work not discounted.

It would seem at first the question of which, if any, of the theories was the correct statement of aperture-to-medium coupling loss could be resolved by experimental measurements. The results of the analyses were sufficiently different that the experiments would show at least definite trends which would agree with a particular theory. Such has not been the case. Each investigator has presented experimental studies which support and justify his conclusions.

Many problems are encountered in attempting to evaluate published experimental work. The aperture-to-medium coupling loss results have for the most part just been passing statements in reports of studies dealing with other questions of tropospheric propagation. The many variable parameters in each of the theories have not been carefully measured, not so much because of a lack of interest or effort, but because of the inability to obtain precise data due to the physical problems. A determination of the atmospheric parameters at any instant is physically impossible. The evaluation of the antenna characteristics, antenna alignment, and circuit details is possible although extremely difficult. Experiments

utilizing 200 to 600 km ranges and large antennas are expensive. The only data available describing the atmosphere for use in analysis is the result of long term measurements such as the 8 years of meteorological data from 45 U.S. weather stations quoted by Bullington (15). The long term aspect of the parameter data and the rapid fading of the received signals on a link force the analysis to consider only the data from extended measurements. And of course if all parameters are not carefully recorded during those extended experiments, the credibility of the results must be suspect. Boithias (22) has listed a set of three requirements he feels are necessary for experiments to be of adequate value: "1) that the free-space antenna gains used be accurately measured, 2) that the recordings of the received signal level on the different antennas should be at least one hundred hours, 3) that the distribution curves for the different received signal levels should be drawn simultaneously for the different antennas under study. In particular it is quite inadequate to know only the distribution law relating to the differences in received signal levels of the two antennas." He continues, "It has to be stated nevertheless that to date few experiments fulfill these indispensable conditions."

In light of the preceding statements casting suspicion on the previous experimental efforts, it would be tempting to ignore them entirely. However to do so would not give a complete picture of the efforts and conclusions drawn on the subject of aperture-to-medium coupling loss.

Rather than attempt to mention all the experimental observations of aperture-to-medium coupling loss beginning with Schott (23) in 1951,

attention will be focused on the attempts to develop an expression from the results accumulated by several authors and refer the reader to the references cited by them for more extensive details. Though several studies are cited repeatedly, the plotted values from those studies sometimes were different. This is not to say there were errors, but that there were questions of interpretation.

The first compilation of experimental data was made by Yeh (24) in 1962. There was a subsequent clarification by Hogg (25) of his results (26), and Yeh corrected the curve in an author's reply at that time. Yeh plotted with θ/α for the abscissa as a matter of convenience. This coordinate was typical for the previous theoretical work and as equal antennas were used in each reference cited, no ambiguity resulted from the definition of α . In 1966, Yeh (27) presented a large collection of experimental results on one graph along with several theoretical determinations (11,15,20,21). The coordinate form changed slightly to $\theta/(\alpha_t \alpha_r)^{\frac{1}{2}}$ where α_t was the transmitting beamwidth and α_r the receiving beamwidth. The determining beamwidth at each end seemed to be the narrower one. Although the loss numbers he plotted were obtained by changing one antenna size no mention was ever made of the other antenna size. Minor corrections or clarifications would only translate the loss points slightly and would not change the final observation. Though he did draw an experimental curve on the graph he concluded, "It can be seen that the theoretical issue of aperture-to-medium coupling loss remains unresolved by experimental data; this is because the experimental data are rather dispersed."

An early hint that experimental points might not solve the dilemma

came from Levatich (28), who suspected the antenna-gain loss was not a simple function of θ/α . He went on to say, "The lack of fit is even more serious for the many diverse theoretical curves, especially when all the data are presented." While citing many of the same works as Yeh he concluded the aperture-to-medium coupling loss appeared to be a monotonic increasing function of (frequency)(antenna diameter)/distance. This variable differed from Yeh's θ/α form by a factor of (distance)⁻² times appropriate constants. Levatich thus found a loss versus distance relationship of inverse form to previous theory and Yeh's experimentally derived curve. Armand and Vvedenskii had published their work showing a loss decrease with increasing distance three years before, but as has been mentioned there were some serious questions about their techniques. The Bullington exponential atmosphere reflection theory showing an expected gain-loss decrease with increasing distance was not published till a year after Levatich's paper.

Shortly after Levatich, Parry (29), ". . . used the data presented by Yeh," (referring to Yeh's paper referenced here as (24)) and arrived at the conclusion

$$L_c \text{ (dB)} = 5.0 + 5 \log_{10}(\theta/\alpha) \quad (12)$$

where α is again the equal beamwidths of the transmitter and receiver. This expression agreed closely with Yeh's curve for $\theta/\alpha \ll 4$ but predicted significantly lower aperture-to-medium coupling loss for larger values of θ/α .

Staras (7) challenged Parry's conclusions and stated, "In any event, all analytic work to date indicates that the exponent of θ/α should be 2 and more probably 3 for large θ/α and not 1/2 as Parry suggests." The exponent of 1/2 on the θ/α term of Parry's expression may be seen by

writing the last term as

$$10 \log_{10} (\Theta/\alpha)^{\frac{1}{2}} = 5 \log_{10} (\Theta/\alpha) \quad (13)$$

Parry replied, in a letter published in January 1964, along with Staras' letter and agreed there was uncertainty due to the lack of data for $\Theta/\alpha \geq 10$. However he concluded, ". . . it seems to be more preferable to use empirical curves which conform with experimental evidence rather than theoretical curves which do not." Neither Staras or Parry had corrected the data in accord with Hogg's letter (24) in 1962. The corrected value did not conform to either conclusion. In Yeh's second compilation (27), where he changed the coordinate slightly by replacing the equal beamwidth α by $(\alpha_t \alpha_r)^{\frac{1}{2}}$ to generalize the form to allow comparison with other data, the last three points for large $\Theta/(\alpha_t \alpha_r)^{\frac{1}{2}}$ were given as 9.0 dB (30) at $\Theta/(\alpha_t \alpha_r)^{\frac{1}{2}} = 3.09$, 0.3 dB (31) at $\Theta/(\alpha_t \alpha_r)^{\frac{1}{2}} = 5.1$, and 14.2 dB (32) at 6.78. No points were observed for $\Theta/(\alpha_t \alpha_r)^{\frac{1}{2}}$ greater than 6.78. These numerical values are included here to place the Parry and Staras exchange in proper perspective. Neither author's allegations have been supported in the range $\Theta/(\alpha_t \alpha_r)^{\frac{1}{2}} > 10$.

Prior to the study reported in this paper only one series of experiments has been conducted for the sole purpose of investigating aperture-to-medium coupling loss. Boithias and Battesti (30) began their measurements in January 1962, and published their findings in September 1964. Their primary conclusions were: 1) aperture-to-medium coupling loss was not a function of distance, and 2) the loss was, to a first approximation, a function of antenna gain only. Equipment limitations allowed them to only compare coupling losses in the range 160 km to 480 km, but not obtain precise numerical values. They observed no differences in

the comparisons in that range. They were able to evaluate coupling losses for three cases and plotted those three values with 12 selected data points from other studies to obtain their loss versus gain curve. Rather good agreement was observed between the points and the composite curve representing them, particularly in the re-evaluated curve presented by Boithias in 1967 (22). However there seemed a definite tendency whenever a range of values was given such as by Chisholm et al. (33), and by Bullington et al. (34), to select the end of the range that fit best.

Boithias and Battesti's results were known and their three points included in Yeh's 1966 compilation from which he concluded there was no experimental decision on aperture-to-medium coupling losses. In fact 13 of the 14 points Boithias used in 1967 were included in Yeh's 40 points.

Dyke (35) summed up the whole theoretical-experimental question, "Most theoreticians find that their experimental data give credence to their theory. This is in spite of the fact that Bullington curves are orthogonal to most other curves, and Boithias finds that coupling loss is independent of distance."

The problem of aperture-to-medium coupling loss has not been solved satisfactorily yet. What is needed is extensive additional data from carefully controlled experiments with attention to measuring and recording all the pertinent information. The first of the two major limitations was given in a call for more work on tropospheric propagation by Mitchell and Fitzsimons (36), "Setting up tropo links solely for the purpose of collecting long-term propagation data is extravagant in cost, time, and

personnel required." They hinted at the second problem by listing six general information areas needed in addition to the three specific ones listed by Boithias: "1) hourly, median, or 10 to 15 minute average values of signals, 2) complete coded sonde data, 3) details of inversion heights, 4) details of constant pressure surfaces, 5) changes in the common volume, and 6) identification of large scale weather changes (frontal passages, monsoon effect, etc.)." If money and personnel were available, there is still a question if it would be possible to record the data needed to specify all the parameters included in the aperture-to-medium coupling loss segment of the tropospheric scatter propagation problem. Continued effort on improving and refining past techniques shows little promise in light of the complete lack of accord observed so far.

Therefore only a totally new and radically different approach would seem to offer much promise. This paper describes such an approach. A system is discussed which fulfills or eliminates each of previously listed nine requirements. The main feature is the massive reduction in size. The immediate inclination to refer to the system as a model is not entirely correct. It does incorporate a length reduction of just over one million and so in that sense is a scale model. But in most respects it is analogous to rather than a model of the conditions found in tropospheric propagation.

Early scaling experiments dealing with radio wave frequencies were limited to a small scale factor as microwave equipment was used for the sources and receivers. Skolnik (37) developed a scale-modeling technique for measuring the radiation pattern of array antennas using 35 GHz to obtain a 27 to 1 scaling over the 1.3 GHz design frequency. With this

scaling he was able to reduce the far-field-measurements distance to 43 meters. Huntley (38) first mentions the use of the helium-neon gas laser as a source to be used with Skolnik's "holey-plate" technique.

Gjessing and Irgens (39) did some scaling work using a white light source and tinfoil reflectors. They shaped the tinfoil in sinusoidal layers and used a lead sulphide photoelectric cell to observe the off-axis field strength. As their work primarily investigated reflection angles from 10° to 65° , the results have little application to more realistic scatter angles of 2° to 6° .

The use of a laser and aperture with a dielectric sphere to evaluate special cases of earth and atmosphere radio wave propagation has been investigated before. Guidry (40) did the initial work in the region near the radio horizon considering only the diffraction mechanism in an "air-less earth" case (gradient of refractive index equal to zero). Subsequent investigation (41,42) with improved techniques and finally a high-power, commercial laser extended the experimental determination of diffraction fields near an "air-less" sphere into the deep shadow area. Excellent agreement with theoretical calculations was shown. The next experiments dealt with scattering and reflection from elevated objects. Several, such as the thin glass rods, had no possible counterpart in the earth-atmosphere case. Other configurations were quite similar to structures shown to exist in the atmosphere (16,19,43,44) and treated theoretically by several authors. The reflection theory discussed by Friis, et al. (6), was experimentally reproduced by various sizes of polished ends of plexiglass rods and copper-plated glass slides (45). The effect of scattering from elevated fluctuations of the refractive

index such as might be caused by turbulence was first treated theoretically by Booker and Gordon (10) and a number of other authors since (11-14). A stream of small glass beads in free fall past the vertical disc was used to simulate elevated turbulent scattering blobs (42,46). The results of those experiments were not compared at that time to published measurements as the form of the height variation of the field strength so conveniently available in laboratory work was almost impossible to duplicate in the atmosphere. Recent discovery of an early work by Trolese (47) allowed comparison of the form of the field intensities as a function of height between the scaled experiments in the laboratory and measurements taken on a range. To obtain his measurements Trolese had built 200 foot elevators at the transmitter and receiver sites to move the antennas continuously from above the radio horizon down into the deep shadow region. Of particular interest was the close agreement in the transition region where the scattered field began to be the dominant term over the diffracted field.

The criteria presented by Boithias (22) and Mitchell and Fitzsimons (36) must be examined in the context of the controlled conditions made available by the scaled experimental setup in the laboratory. All requirements for numerous data samples over a long time period stem from the variations of the atmosphere with time and major changes in meteorological conditions. A large number of points are needed to remove the time variations and specify the effects of the meteorological changes. The experiment fulfilled these limitations by utilizing a propagation path which did not change major properties and then time averaged the effects of the small structure variations. The need for constant and careful

monitoring of the meteorological conditions was met by knowledge of the scattering media used. The free-space gains of the apertures were accurately measured as requested by Boithias.

However the experimental technique does have a limitation which must be considered in the application of the results. The propagation path cannot be a precise representation of the atmosphere for two reasons. No exact description has been written of the atmosphere which has received more than cautious, limited acceptance. If any of the atmospheric descriptions were completely valid, the theories based on those specifications would have been confirmed by experimental data. Again such has not yet been the case. Secondly the physical problems involved in building propagation paths in the laboratory which incorporate small gradients in the refractive index in agreement with the theoretical assumptions have not yet been solved. Consequently the propagation path employed was a compromise between an ideal representation of a particular theory and the physical limits of construction.

EXPERIMENTAL DESIGN

Transmitter

A helium-neon gas laser was used as a source of high power density, monochromatic, linearly polarized, coherent, plane waves to illuminate the transmitting aperture. The beam was focused and collimated by two short-focal-length lenses which increased the power density. The beam diameter was still large compared to the transmitting aperture. More extensive discussions of the details of the source have been presented previously (41,42,45,46).

The transmitting aperture was a 200 micrometer (316 wave lengths) diameter circular hole in a platinum slug. The aperture was originally intended to be used in an electron microscope. The transmitting aperture was mounted in a specially constructed frame held against a pyrex disc. The height of the aperture was 1.25 mm above the disc. The transmitted beam was aimed each time with the edge of the central maximum just tangent to the surface. The visible beam of the helium-neon laser was immeasurably easier to align than a beam of some other wavelength.

Propagation Path

Figure 2 is a schematic of the major components of the experimental setup in their relative positions. The spherical dielectric surface used in the experiment was a pyrex disc ground to a 5.5 m spherical radius of curvature. It was originally used by Guidry and is discussed at length in his paper (40). Only a brief summary of the properties will be included here.

The disc was constructed of two sheets of 1 1/4 inch thick

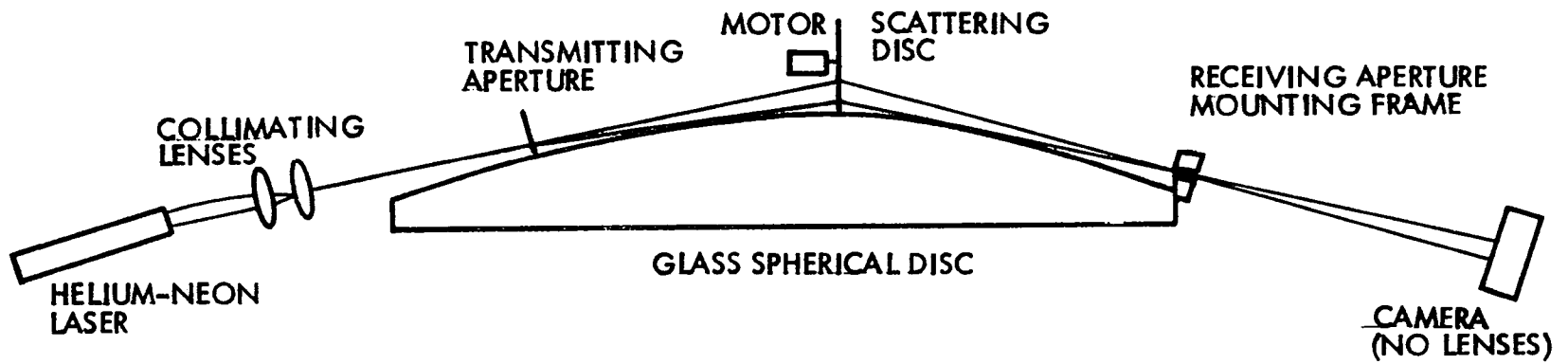


Figure 2. Schematic of experimental setup (not to scale)

commercially annealed #7740 pyrex, 60 cm in diameter, bonded together with black epoxy cement. The 5.5 m radius curvature was held to a tolerance of about $1/4 \mu\text{m}$ in any 15 cm region. The constitutive parameters for pyrex at optical frequencies are $\epsilon_r = 1.474$ and $\sigma \approx 0$. The pyrex disc was suspended vertically in a sling with three spring-loaded contacts to position it about two axes.

The volume above the disc was considered to have no effect on the beam as it was best described as still, clean air. The room was kept as dust-free as possible and all experiments carried out in a curtained enclosure. The curtains cut out any stray background light and minimized any air motion or turbulence. Thus the gradient of the refractive index in the volume near the disc was zero.

Several different scattering media were evaluated before the final selection was made. The free falling spherical glass bead stream used in some earlier work (42,46) was rejected due to the inconvenience of re-loading the system for the approximately 250 tests that were required in the final analysis for this study. Also any increase in humidity caused the beads to cluster and the flow became uneven. A fixed scattering media constructed of the beads mounted on a glass slide was quite simple to use but was finally rejected. The scattering media selected was constructed using a 1/16 inch thick disc of plexiglass, 6.7 cm in diameter, coated on one side with the glass beads. The scatter disc was mounted on the shaft of a small motor and rotated at 13 650 rpm during each test.

The beads were of high-grade optical crown glass, soda-lime type, with an index of refraction within the range of 1.50 to 1.55 and free from all surface films. The size guaranteed was 90 percent population in

the 10 to 30 μm diameter range. Microscopic evaluation of a sample showed a mean of 24.0 μm (38λ) and a standard deviation of 3.64 μm . The beads were held to the disc by a very minute amount of a silicon-base belljar grease. After a little practice it became routine to apply a quite even covering of beads. Microscopic study of the actual bead distribution used throughout the final experimental determinations showed it could be described by 90 percent completion of the first layer, 20 percent completion of the second possible layer, and 1 percent completion of the third layer.

The scatter disc was positioned at mid-range for each of the determinations. It was aligned normal to the beam by positioning the disc so the reflection from the smooth surface on the transmitter side of the disc fell directly on the transmitting aperture. The vertical position was fixed by the need for clearance between the spinning disc and the spherical surface. The scatter disc was accurate enough allow the clearance to be held in the neighborhood of 0.25 mm.

As the maximum main lobe dimension to the first null on each side was approximately two millimeters, only a narrow band of beads at the edge of the scatter disc was in the beam.

The four range distances evaluated were at 26.0 cm, 34.8 cm, 43.4 cm and 52.0 cm which corresponded to distances of 300 km, 400 km, 500 km, and 600 km on an earth size sphere when one considered the 1.16×10^6 length scale factor.

Receiver

The receiving apertures consisted of a set of platinum slugs having diameters of 50, 100, 200, 400 and 750 μm or 79, 158, 316, 632 and 1185 wavelengths respectively. The receiving aperture mounting frame was specially designed to allow three degrees of translational motion and two degrees of rotation. The slugs were housed in a slide which had been notched for detent ball location and then drilled in place to accept the 2.3 mm diameter slugs. The technique insured the positioning of each aperture so that only the diameter of the aperture would change when the receiver was switched from one size to the next. An additional precaution was to cycle through the apertures in the same order each time.

The alignment of the receiving apertures was accomplished in five steps. The mount was moved up to center the aperture in the beam from the transmitter (scatterer removed). The mount was rotated about its two axes until the beam was reflected back onto the transmitting aperture by a mirror attached to the slide and parallel to the plane of the apertures. The scattering disc was positioned as described earlier. The scattering angle was computed and the mount rotated to position the plane of the apertures normal to a ray from the center of the main beam on the scattering media to the center of the aperture. The mount was then translated back to its position 1.25 mm above the spherical surface. The procedure was repeated for each range studied.

Recording System

The previously published analyses (40-42,45,46) were obtained by placing sheet film at the edge of the spherical disc, normal to the

surface, and exposing the film directly. The technique worked well and was capable of recording the diffracted and scattered fields over significant height ranges. The evaluation of aperture-to-medium coupling loss obviously required the addition of a receiving aperture to the set. The electron microscope apertures presented a reasonable solution. However it was then necessary to develop a way to determine the power received by the apertures. The quantity of interest was the total power received by the aperture, not the power density distribution as had been desired before.

Large apertures of many wavelength diameters have a relative efficiency of unity (48). Thus analysis of the power available through an aperture would also yield the power available at the aperture. Therefore attention was directed to evaluating the power transmitted through the receiving apertures.

A possible measurement system was to use a photomultiplier tube. However extensive attempts over a long period of time showed its apparent advantage of reacting to total power (light incident on the photocathode) was not realized. Repeated experiments failed to give sufficiently consistent results to warrant acceptance of the results. Several problems contributed to the failure of the photomultiplier tube, in particular "hot spots" in the photocathode and insensitivity in the 6328 Å wavelength region of the laser source. Calibration of the output current to give even relative power readings proved difficult let alone attempting to extend the range of useful power measurements to encompass the values expected. The photomultiplier tube approach should be considered again if tube developments overcome these limitations. The use of a

photomultiplier tube operating "as advertised" would enormously simplify and facilitate the collection of data.

The technique constructed to measure the total power through the apertures was reasonably simple in concept but complicated in execution. The light energy through each of the receiving apertures was recorded on Plus X photographic film. A high quality 35 mm camera with the lenses removed was used to hold the film and to set exposure times. Data for each range evaluated consisted of three cycles through the receiving apertures and three to five different exposure times for each of the five receiving apertures per cycle plus three different exposure times for the range reference films. The films were then scanned and the power measurements were available through calibrations of the scan output. As the purpose of the project was to obtain a system capable of yielding numerical results rather than just a generalized form of the solution, the details of the analysis merit elaboration here.

Photographic film reacts to the total exposure to which it is subjected. The exposure value is defined as the intensity of the light energy incident on the film times the time period the film is subjected to that light. The density of the "negatives" produced by developing the film is defined as

$$D = \log_{10} \left(\frac{100}{\text{percent transmission through the film}} \right). \quad (14)$$

The density of a particular film is determined by the constants of the film type used and the exposure value incident on it.

$$D = \gamma (\log_{10} \text{Exposure} - \log_{10} C) \quad (15)$$

where D is density, γ is film reaction coefficient and C is an emulsion

constant (49).

Figure 3 shows a density versus exposure curve for a typical film. The value of γ is the derivative of the density-exposure curve. A differential form of the expression may be used to specify an "effective γ " or a piecewise linear approximation for γ evaluated between arbitrary points 1 and 2.

$$\gamma_{12} = \frac{D_2 - D_1}{\log_{10} \text{Exposure}_2 - \log_{10} \text{Exposure}_1} \quad (16)$$

The straight line portion in Figure 3 has a constant γ and is considered the best operating range. A constant γ throughout the operating range of an experiment is convenient but not necessary. The anorthophotic emulsions do not have a straight line segment (γ equals a constant) in their characteristic curve or may have two (two different constant values of γ). The value of γ is often not a simple function such as the constant values described so far. In fact a common phenomenon called solarization (49) is characterized by negative values of γ at extremely high intensities.

The actual γ for Plus X exposed to red light (6328 Å wavelength) is shown in Figure 4. The values for γ are plotted as a function of density instead of the expected exposure ordinate. The reason for this form will become apparent as the format for the calculations is derived.

Substituting the definition of exposure (Exposure = Intensity (In) times time (t)) yields

$$\gamma_{21} = \frac{D_2 - D_1}{\log_{10} I_2 t_2 - \log_{10} I_1 t_1} \quad (17)$$

Changing any combination of intensities and times and determination of the resulting densities produces the γ for that range. Measurement of an

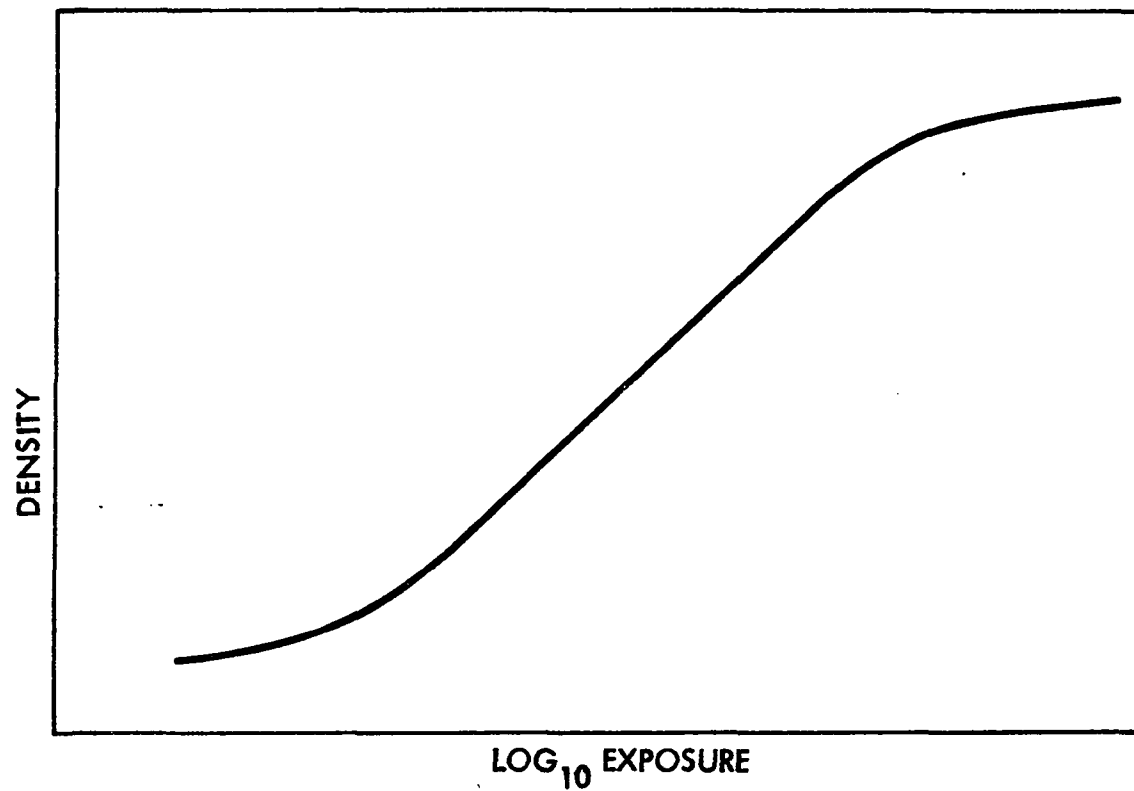


Figure 3. Density versus exposure for a typical film

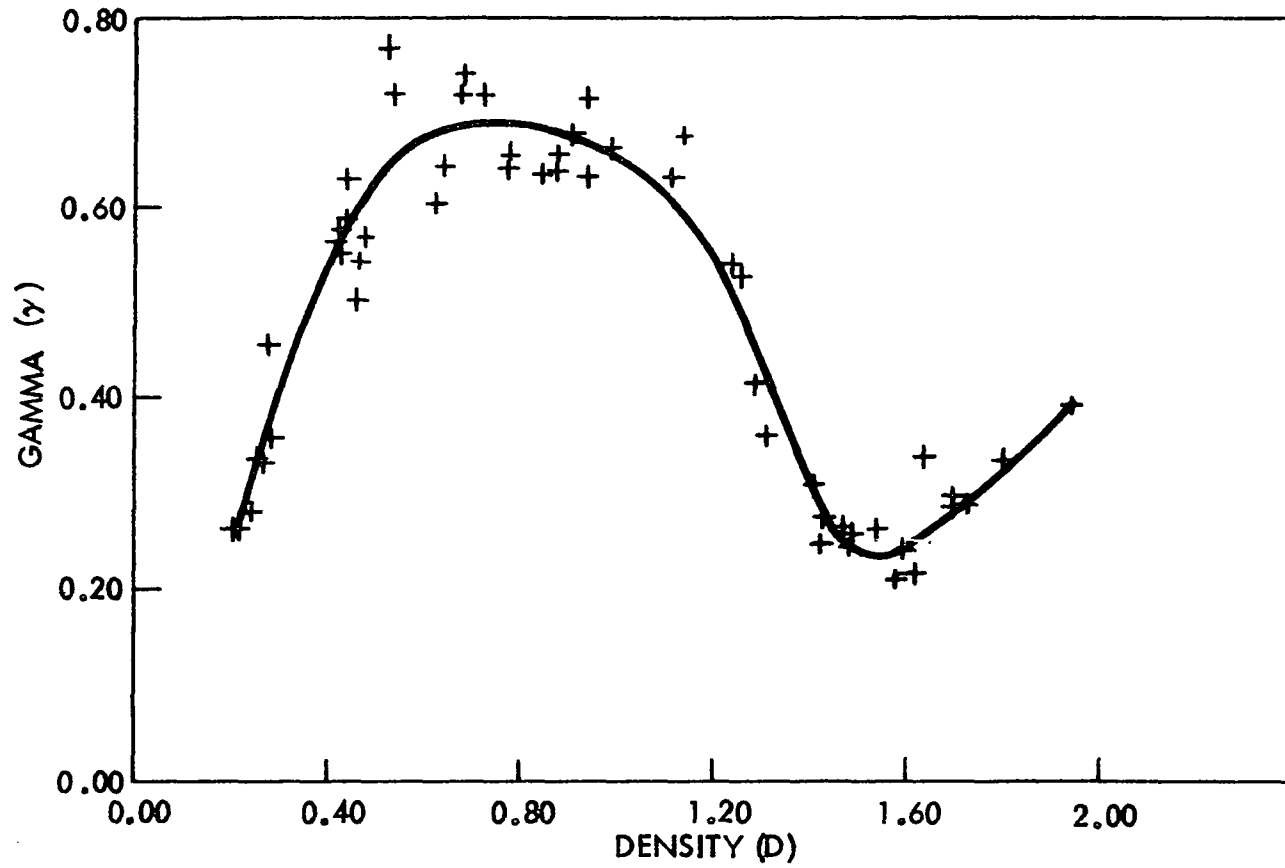


Figure 4. Actual gamma versus density curve observed for Plus X film exposed by red light

intensity change in the laboratory was not as accurate as setting the time periods. In fact the time change method would have been selected anyway as there is a slight breakdown of the reciprocal relationship of intensity and time (49) due to the practical aspects of the emulsion reaction. Glafkides states the γ will remain more constant for varying times than for varying intensities. The curve shown in Figure 3 was determined by using Equation 17 ($\ln_2 = \ln_1$) in the form

$$\gamma_{12} = \frac{D_2 - D_1}{\log_{10} \frac{t_2}{t_1}} \quad (18)$$

Density measurements were made with a recording microphotometer. The recorded values were related to the film density by

$$D = (-C_2)(\log_{10} SR) + C_3 \quad (19)$$

where SR is the scale reading and C_2 and C_3 are appropriate constants. The constants C_2 and C_3 changed slightly from day to day so it was necessary to recalibrate the instrument before each run with a calibrated step tablet. Repeated checks during and after runs indicated the machine seemed to be operating within its specifications: reproducibility, $\pm 1/2$ percent; linearity, ± 2 percent; clear plate drift, ± 1 percent in 30 minutes; zero drift, $\pm 1/2$ percent of full scale in 30 minutes. The microphotometer was rated over a density range of 0 to 3.5 or better.

The techniques used in previous work to evaluate field intensities were extended to yield numerical determination of total power incident on the film. Starting from the definition of exposure,

$$\text{Exposure} = (\text{Intensity})(\text{Time}), \quad (20)$$

multiplying both sides by an area term and exchanging power density for

intensity gives

$$(\text{Exposure})(\text{Area}) = (\text{Power Density})(\text{Area})(\text{Time}) \quad (21)$$

Equipment limitations forced the analysis to be in terms of differential areas and a summation of the results for each area.

$$(\text{Exposure}_i)(\text{Area}_i) = (\text{Power Density}_i)(\text{Area}_i)(\text{Time}) \quad (22)$$

Time is not subscripted as it was a constant for each summation which covered only one film. In terms of a total power (p),

$$(\text{Exposure}_i)(\text{Area}_i) = pt \quad (23)$$

The piecewise linear approximations for the values of γ were used to determine Exposure_i as some multiple (v_i) of a reference Exposure_0 . This was accomplished by rewriting Equation 16 in a differential form as

$$\log_{10} \frac{\text{Exposure}_i}{\text{Exposure}_{i-1}} = \frac{D_i - D_{i-1}}{\left(\frac{\gamma_i - \gamma_{i-1}}{2}\right)} \quad (24)$$

The increments in this compilation of the graph constructed to yield Exposure_i directly from D_i measurements were selected as $D_i - D_{i-1} = 0.04$ to obtain a reasonable compromise between ideal precision and realistic data reduction. The procedure is illustrated by summation of both sides of Equation 24 to the form

$$\log_{10} \frac{\text{Exposure}_i}{\text{Exposure}_0} = \sum_{j=1}^i \frac{D_j - D_{j-1}}{\left(\frac{\gamma_j - \gamma_{j-1}}{2}\right)} \quad (25)$$

In terms of the multiple v_i , Equation 25 was written as

$$\log_{10} v_i = \sum_{j=1}^i \frac{D_j - D_{j-1}}{\left(\frac{\gamma_j - \gamma_{j-1}}{2}\right)} \quad (26)$$

With a method developed to determine the numerical value of v_i , it

was useful to rewrite Equation 23 as

$$(v_i \text{ Exposure}_0) (\text{Area}_i) = pt \quad (27)$$

Comparison of power totals of two different films representing two different test measurements was accomplished by comparing their respective versions of Equation 27 (subscripted as 1 and 2).

$$\frac{\sum_{i=1}^{N_2} (v_{i2} \text{ Exposure}_0) (\text{Area}_{i2})}{\sum_{i=1}^{N_1} (v_{i1} \text{ Exposure}_0) (\text{Area}_{i1})} = \frac{p_2 t_2}{p_1 t_1} \quad (28)$$

All Area_i terms were held equal throughout the study by the data reduction techniques. Equal sized sample populations for comparison were assured by setting Exposure_0 to correspond to very nearly the background density of the film and noting that $v_i = 1$ for all areas having a density value at or below that threshold. Thus with N equal to the larger of N_1 or N_2 ,

$$\frac{p_2}{p_1} = \frac{t_1}{t_2} \frac{\sum_{i=1}^N v_{i2}}{\sum_{i=1}^N v_{i1}} = \frac{t_1}{t_2} \frac{V_2}{V_1} \quad (29)$$

The v_i terms were evaluated from the chart records by compiling graphs relating v_i as a function of density (see Equation 26) to the chart readings (see Equation 19). Direct evaluation of each v_i was thus possible from the chart scale reading for each sample point. The graphs were rederived for each recalibration.

A rectangular slit $10 \mu\text{m}$ by $200 \mu\text{m}$ was used for all samples included in the study. Scanning rate across the film was 5 mm per minute. The

positional accuracy specification of the microphotometer was $3\mu\text{m}$ over the 200 mm range with a periodic error of less than $1\mu\text{m}$. Data points were read from the charts at intervals corresponding to $166\mu\text{m}$ along the films. As the slit width was $10\mu\text{m}$, the sample areas did not overlap. The sampling interval was selected to be a compromise between ideal precision and reasonable data reduction. It was particularly convenient as the chart speed was 30 divisions per minute or 6 divisions per mm of film travel. The film density points were read at each chart division line and converted to v_i terms for summation. No attempt was made to position the sample points relative to peak or threshold or to the sample points of the adjacent sweep. The sweeps were made at $200\mu\text{m}$ increments corresponding to the $200\mu\text{m}$ dimension of the scanning slit. An analysis of the number of data points per film record showed a mean value of 201 points. Experimental verification of the accuracy and repeatability of the random placement of the sample grid in each sweep was accomplished in both a large sample space and a "worst case" small sample number. Films were rescanned at the beginning and end of a run and their V totals compared. The totals agreed within 2.35 percent for the greatest difference and half the comparisons were within 0.73 percent. The small sample number test was to take one narrow, highly-peaked sweep and vary its position on the chart through a cycle of eight equally spaced positions one eighth of a chart division apart. The V_i ranged from 60.1 to 61.6 with a mean of 60.75 and a standard deviation of 0.45 or 0.74 percent of the mean.

The size of the power distribution on the film was a function of the receiving aperture size and the film distance from the receiver. Goodman (50) showed the peak power density for a circular aperture to vary as

$(b^2/z)^2$ where b is the aperture diameter and z the distance to the observation point. Comparison of two different combinations was

$$\hat{p}_2 = \hat{p}_1 \left(\frac{b_2}{z_2}\right)^2 \left(\frac{z_1}{b_1}\right)^2 \quad (30)$$

where \hat{p} represents power density. The radius terms determining each area were given by $z_i \alpha_i / 2$ where α_i was the beamwidth of the pattern ($1/b_i$ relationship). The areas included in a circular beam cone at distances z_1 and z_2 were thus related as

$$\text{Area}_2 = \text{Area}_1 \left(\frac{z_2 b_1}{z_1 b_2}\right)^2 \quad (31)$$

The power totals for one aperture size (b) and two different distances (z_1 and z_2) were related as

$$p_2 = \hat{p}_2 \text{Area}_2 = \hat{p}_1 \left(\frac{z_1}{z_2}\right)^2 (\text{Area}_1) \left(\frac{z_2}{z_1}\right)^2 = p_1 \quad (32)$$

Thus the total power results were not only insensitive to small errors in z during the experiment, but theoretically any z or combination of z 's would have given the same results. However even with the non-linearities of the film carefully allowed for, the best results would be obtained by holding the exposure patterns, both size and intensity, as identical as possible.

The most critical feature of an experiment should be the one most accurately controlled. In this system the critical time intervals were easily set and reproduced by the camera timing system. The time response is most easily shown by starting from the desire to have equal area patterns on the film. For a change of $b_2 = 2b_1$ of the receiver aperture

typical of the experiment, $z_2 = 2z_1$ to hold the areas equal. Substituting into Equation 30,

$$\hat{p}_2 = \hat{p}_1 \left(\frac{(2b_1)^2}{2z_1} \right) \left(\frac{z_1}{b_1} \right)^2 = 4\hat{p}_1 \quad (33)$$

With $\hat{p}_2 = 4\hat{p}_1$ and equal areas, equal exposures were obtained by holding $t_2 = t_1/4$.

Recopying Equation 29 and substituting $t_2 = t_1/4$,

$$\frac{p_2}{p_1} = 4 \frac{V_2}{V_1} \quad (34)$$

For the case described and the theoretical result of doubling the aperture producing four times the power, $V_2 = V_1$ and $p_2 = 4p_1$. This was observed experimentally as described in the Experimental Results section of this paper.

So by arranging the experiment to produce comparable V_2 and V_1 , the ratio of power available in the two cases is dominated by the time ratio, which is again, the simplest parameter to work with.

The times were implemented by use of the camera internal shutter control for short exposures and a laboratory timer for the long exposures (4 and 16 seconds). The actual timing of the camera shutter was measured. These times were quite repeatable and were used in all calculations in place of the nominal shutter times.

The distance and time ratios actually used in the study followed the pattern established in the preceding paragraphs with two exceptions. The longest exposure time which could be used was 16 seconds. The next time increment at 64 seconds could not be used due to a slight increase in the

background density caused by the stray leakage light, and the fact that the motor spinning the scattering disc would heat up rapidly after about 10 seconds. The distances were limited by a wall to about 1 meter maximum and the depth of the aperture mount and camera frame limited the minimum to 10 cm.

In the section describing the propagation path, the choice of a rotating, bead-covered disc for the scattering media was given without justification. Now that the details of the receiver and recording system are available, the reasons for the disc selection may be presented in detail.

The experiments with the fixed, bead-covered slide did not give repeatable results because the fine structure of the scattered field was of comparable size to the receiving apertures. The form of the power distributions on the film varied from test to test. Any minute movement of the receiver or the scattering media would shift the observed pattern to a similar but obviously different distribution.

Long term recording of tropospheric radio waves and determination of a mean value was the solution to this problem employed by other investigators. As the atmosphere shifted through its various possible structures, the recorders time-averaged the effects and a statistical statement of the atmospheric effects was produced. The laboratory analog was the rotating disc which changed the instantaneous scattering media through its entire range of values each revolution. The requirement of 100 hours of recording radio wave signals proposed by Boithias was equivalent to the laboratory requirement of a good statistical sample of the possible configurations of the scattering media. The rotating disc

bead distribution very effectively met this requirement. Examination of the worst case (maximum beam diameter incident on the beads and minimum time exposure) showed approximately 119 complete "changes" of the scatterers in the transmitter beam. That is to say a particular point or bead required 1/119 of the total test time to pass clear through the incident beam. In the case of the longer exposures there were up to about 95 000 "changes" of the beads. Of course these were not all different due to the fact that one revolution of the disc completed one cycle through the possible configurations.

Super 8 movie films were made of the scattered signal through the receiving aperture. No attempt was made to obtain quantitative results from the movies. They were useful in observing the transition of the observed patterns from the stationary scatterer to the time averaged patterns from the revolving scatter disc.

EXPERIMENTAL RESULTS

Aperture-to-medium coupling loss as defined and discussed deals with the realization of less antenna gain than expected. To treat it experimentally, the expected antenna gain must be determined.

The gain in dB of a large circular aperture is given by Silver (51),

$$G = 10 \log_{10} \left(\frac{\pi^2 b^2}{\lambda^2} \right) \quad (35)$$

The increase in antenna gain due to doubling the diameter was calculated as

$$G = 10 \log_{10} \frac{b_2^2}{b_1^2} = 20 \log_{10} \left(\frac{2b_1}{b_1} \right) = 6.020 \text{ dB.} \quad (36)$$

All single steps in the evaluation were to double the diameter except the 400 μm to 750 μm case (632 to 1185 λ) where the calculated gain increase was

$$G = 20 \log_{10} \frac{750}{400} = 5.460 \text{ dB.} \quad (37)$$

Gain calculations always assumed plane wave illumination in a free-space configuration. The experimental apertures were positioned in the center of the transmitted beam, and the gain increase between apertures evaluated. The results are tabulated in Table 1.

The close agreement between the calculated gain increases and the actual gain increase tended to lend confidence to the experimental determination as numerous experiments have verified experimental versus theoretical agreement for free-space conditions. All factors had to be correct for such close correlation to be observed again. The measured gain increases were used in all determinations of aperture-to-medium

Table 1. Antenna gain increases, calculated and observed

Apertures compared	Calculated gain increase (dB)	Actual gain increase (dB)
50-100 μm	6.020	5.962
100-200 μm	6.020	6.650
200-400 μm	6.020	6.000
400-750 μm	5.460	6.140

coupling loss of course.

A range-power film was included in each set of test films at each range. One of the purposes of the range-power film was to indicate alignment errors that might affect the test results. The range film was obtained by moving the receiving aperture up into the beam exactly as was done in the antenna gain increase determination. If the transmitting aperture was illuminated identically the range power films would have shown only the $1/d^2$ attenuation of power density which is characteristic of a free-space field. The 50 μm aperture (79λ) was used each time. The time base was limited to 1/1000 second minimum so any of the larger apertures allowed greater exposure value than the dynamic range of the film could handle with proven accuracy. Small errors in alignment would cause variations from calculated attenuation due to range distance changes. However unless the errors were large enough to cause the test results to fall outside the working range of the recording techniques, they would

not affect the results of the tests at all. The observed range attenuation values showed the transmitted power was always well within acceptable limits.

The sequencing program produced three independent sets of films for each receiving aperture at each range. The films were selected from each set in accord with the previously discussed time change versus aperture change criteria. The reason for shooting the films in sets of exposure times was to insure at least one film would be in the operating range of the analysis technique.

The selected films consisting of one film for each aperture for each cycle through the apertures for each range plus the range attenuation films were scanned and tabulated. A numerical check of the reproducibility of the results was accomplished by averaging the three films for each of the aperture-range combinations and dividing the three by this average. Obviously this compilation would yield an ensemble mean of the 58 films of 1.00. One standard deviation was only 0.0538 however, thus demonstrating the reproducibility of the results. Only 58 films were used as two of the 60 expected showed the aperture had not been changed from the previous size.

Most published theories and discussions of aperture-to-medium coupling loss (1,4-7,10,11,13-15,20,24,27-29,35) incorporate a variable of the form $f(\theta, \alpha) = g(\theta)/h(\alpha)$ where g and h are not constants. Implicit in their forms is the understanding that all combinations of θ and α which produce the same $f(\theta, \alpha)$ would have the same aperture-to-medium coupling loss. Also a change in $f(\theta, \alpha)$ may be caused by a variation of θ or complementary variation of α and the same change in L_c would be observed.

Attempts to plot the values of ΔL_c measured in the laboratory versus any of the $f(\theta, \alpha)$ -form variables used previously resulted in a scattered set of points with no general form let alone any precise correlation. Thus the laboratory findings have been separated into two sections to properly describe the findings. The compound changes in $f(\theta, \alpha)$ to cause an incremental aperture-to-medium coupling loss term have been replaced by changes in only one variable. The additional descriptive terms of aperture-induced and distance-induced seem a little cumbersome but are necessary for clarity in the discussion.

The definition of antenna gain compared the power density function of the antenna with the uniform power density of an isotropic radiator. Experimentally it was impossible to compare the transmitting and receiving apertures with an isotropic radiator since such a radiator cannot be realized. Thus the observed gain increase terms given in Table 1 are only gain change terms. If any one of the gain terms were known, the observed gain differences would specify the gains of the remaining apertures. Though discussed only by Hartman (4) and Gough (5) "change in gain" must be the form of all experimental results. The particular choice of reference aperture would not change the conclusions of the study in any way. The 200 μ m aperture was selected as the reference here only to facilitate the display and analysis of the data.

Figure 5 shows the observed relative power for the 26.0 cm range. The values are plotted versus the aperture diameter given in wave lengths. A slightly different form of the data obtained by compiling the incremental aperture-to-medium coupling loss (ΔL_c) as given by Equation 8. That is to say the aperture-induced incremental aperture-to-medium coupling

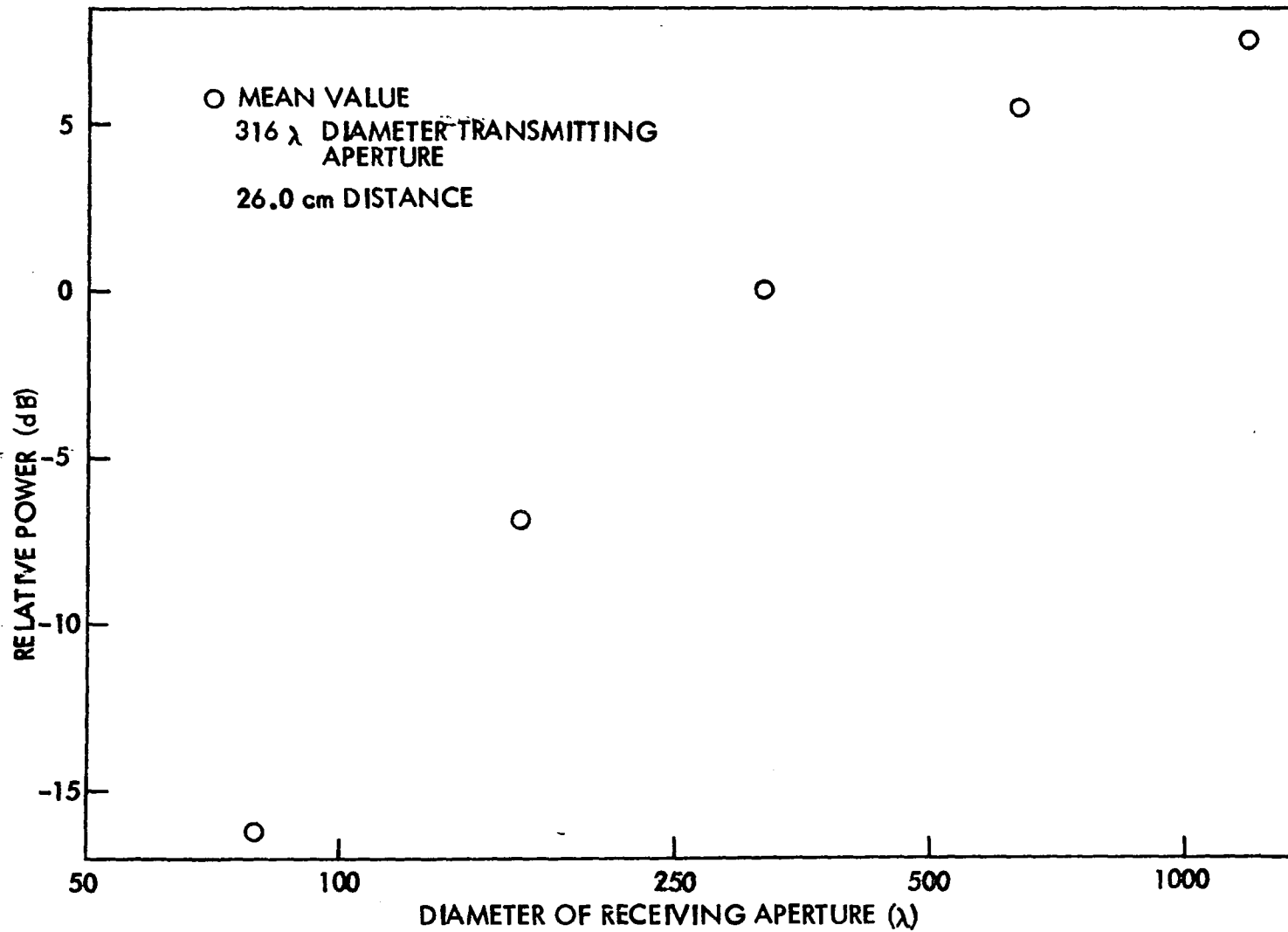


Figure 5. Relative power observed versus diameter of receiving aperture

loss is equal to the measured increase in free-space gain minus the measured increase in gain for the actual propagation path. The values of ΔL_c for the 26.0 cm range are plotted in Figure 6. Figures 7, 8, and 9 are the graphs of the aperture-induced incremental aperture-to-medium coupling loss observed for the longer ranges of 34.8 cm, 43.4 cm, and 52.0 cm respectively. Figure 10 is a graph showing the mean ΔL_c terms for the aperture changes evaluated at each range. Plotted with them is a solid curve delineated by

$$\Delta L_{ci} = 18 \left| \log_{10} \frac{b_t}{b_i} \right| 2.50. \quad (38)$$

where b_t is the diameter of the transmitting aperture and b_i is the diameter of the receiving aperture. The difference in aperture-induced incremental aperture-to-medium coupling loss for aperture changes may be determined by evaluating ΔL_{c2} and ΔL_{c1} and subtracting. The actual gain increase due to a receiving aperture change is the measured free-space gain increase minus the difference in incremental aperture-to-medium coupling loss determined for those two apertures.

The trend of loss increasing as the aperture gain increased was present in the experimental results for apertures larger than the transmitter. For apertures smaller than the transmitter, the loss was observed to decrease as the aperture gain increased. Two representative examples from the experiment illustrate those trends. Taking a change from the 632λ diameter aperture to the 1185λ diameter aperture as the first example:

$$\Delta L_{c2} = 4.06 \quad (39)$$

$$\Delta L_{c1} = 0.80 \quad (40)$$

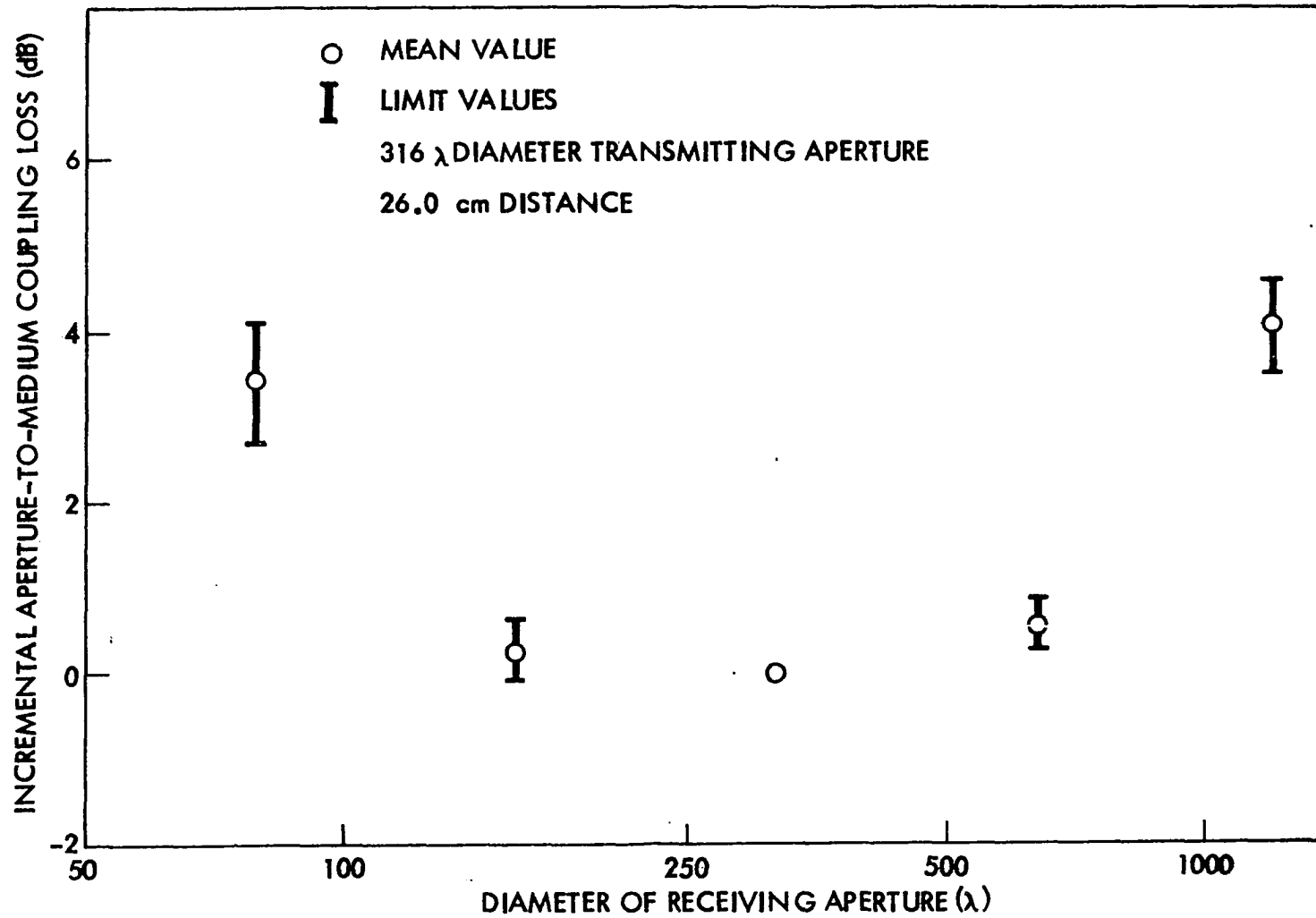


Figure 6. Aperture-induced incremental aperture-to-medium coupling loss for 26.0 cm range

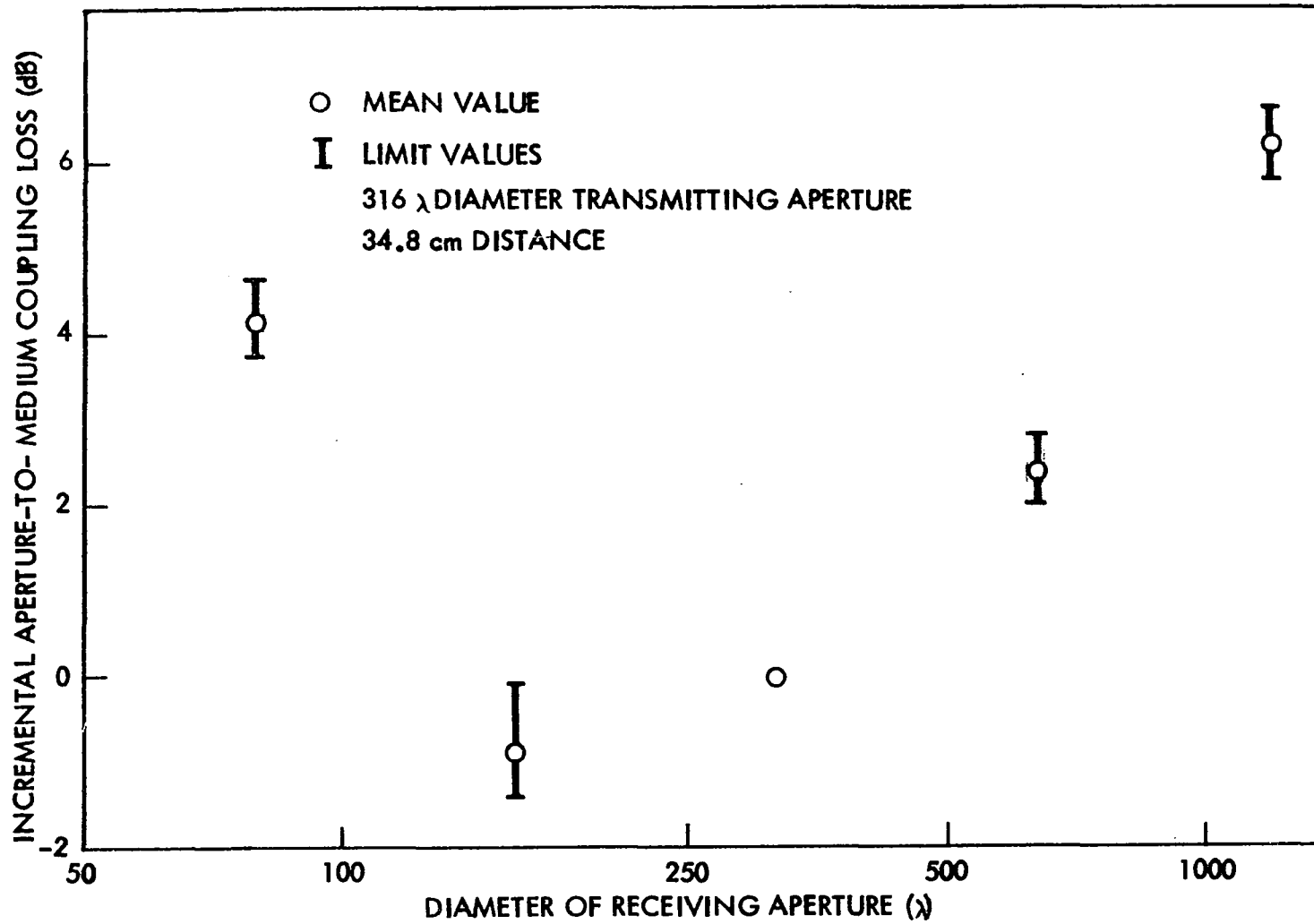


Figure 7. Aperture-induced incremental aperture-to-medium coupling loss for 34.8 cm range

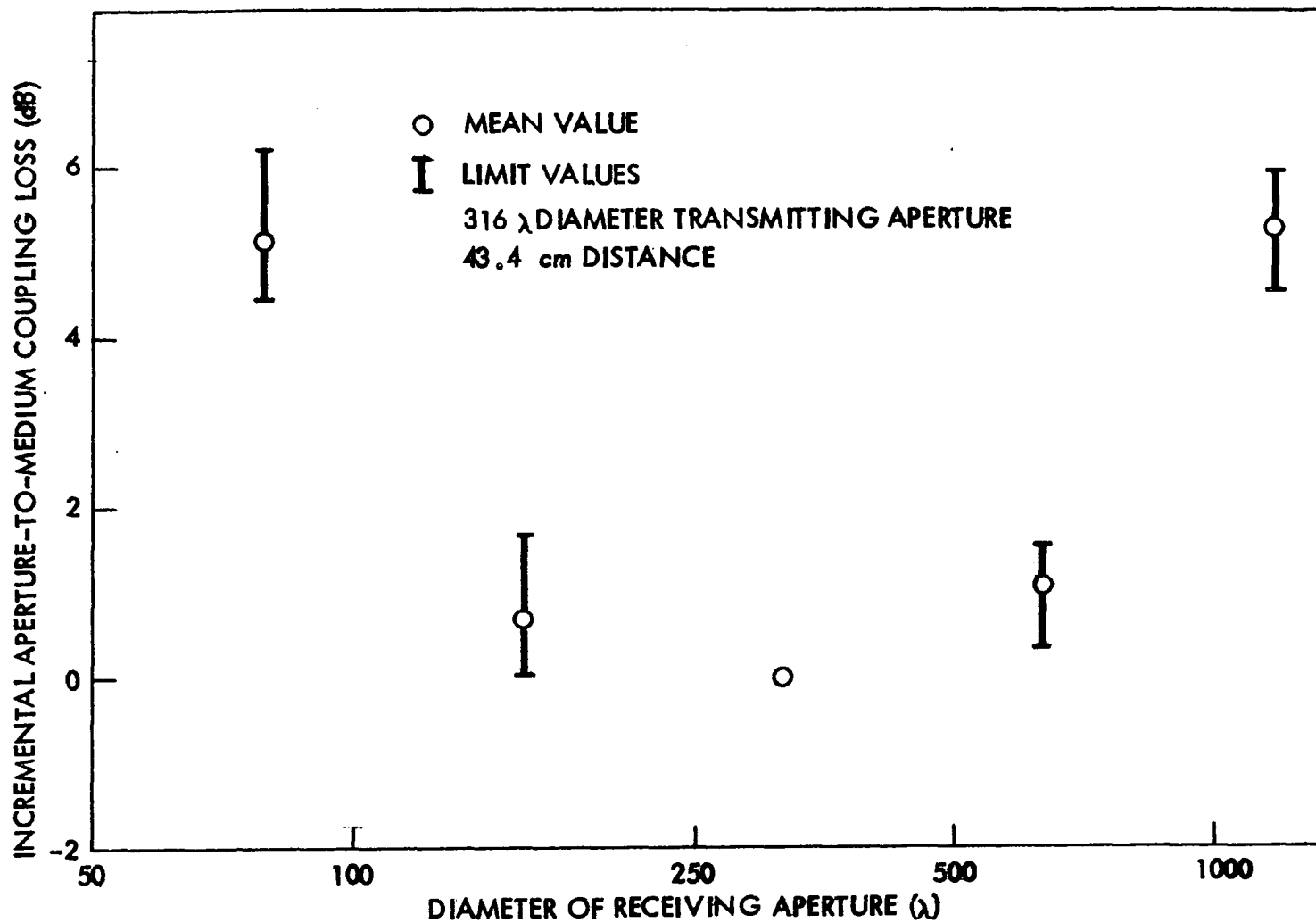


Figure 8. Aperture-induced incremental aperture-to-medium coupling loss for 43.4 cm range

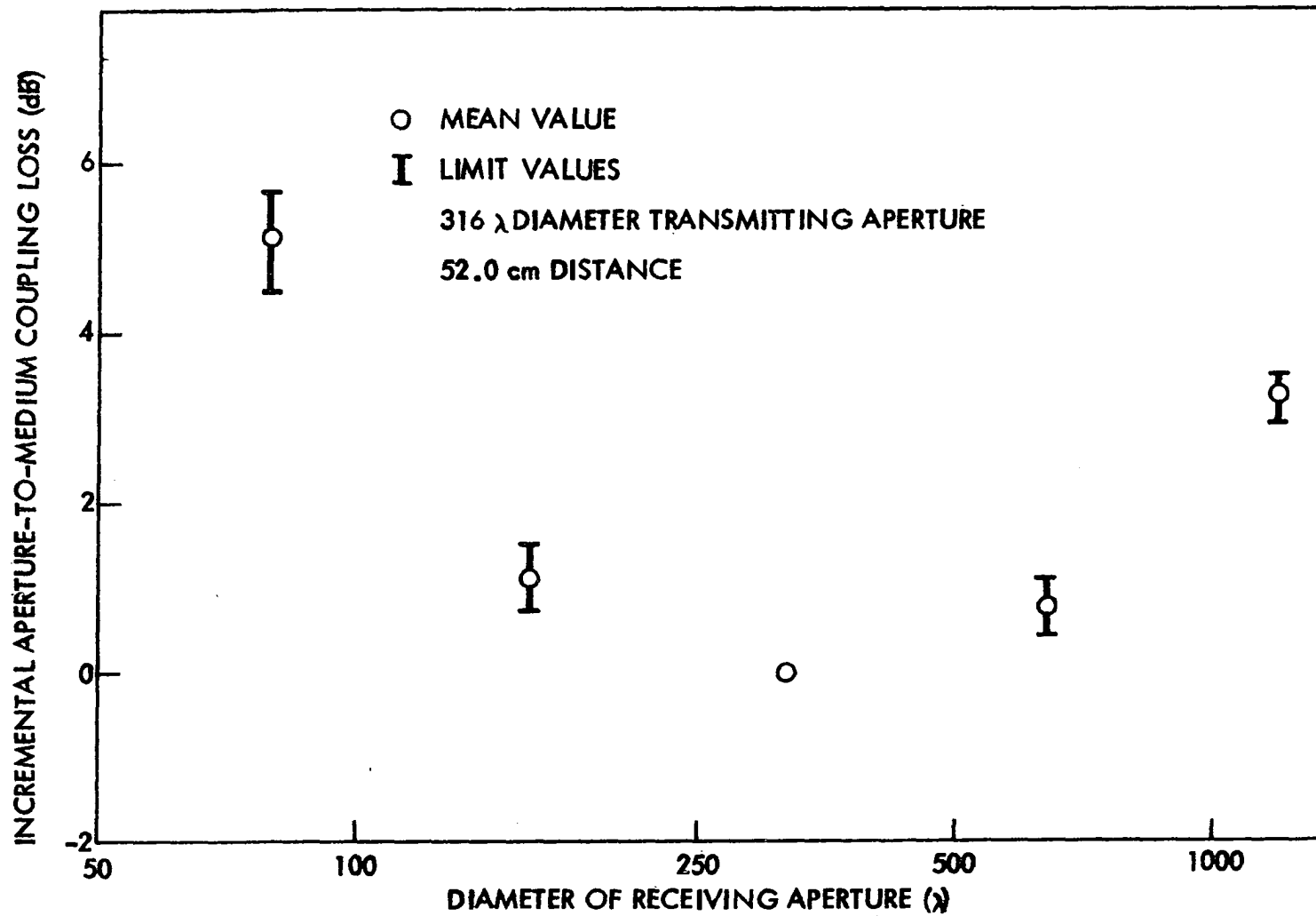


Figure 9. Aperture-induced incremental aperture-to-medium coupling loss for 52.0 cm range

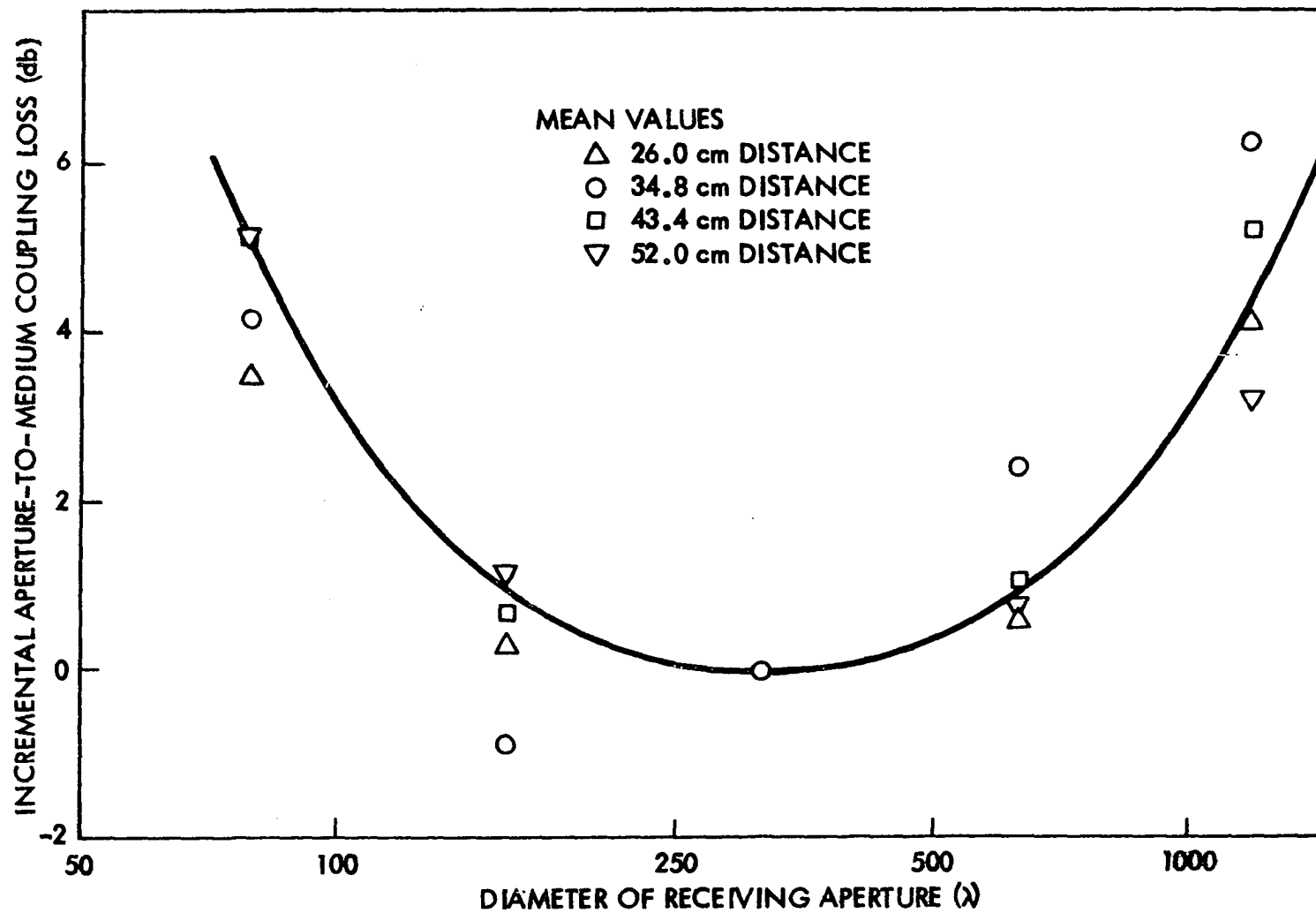


Figure 10. Aperture-induced incremental aperture-to-medium coupling loss

$$G_{1185\lambda} - G_{632\lambda} = 6.14 \text{ dB (observed),} \quad (41)$$

gives an actual gain increase of

$$6.14 - (4.06 - 0.80) = 2.88 \text{ dB.} \quad (42)$$

The second trend is shown by the change from the 79λ diameter aperture to the 216λ diameter one.

$$\Delta L_{c2} = 0 \quad (43)$$

$$\Delta L_{c1} = 4.52 \quad (44)$$

$$G_{316\lambda} - G_{79\lambda} = + 12.61 \quad (45)$$

Substituting into the same expression of measured free-space gain increase minus the difference in incremental aperture-to-medium coupling loss gives

$$+ 12.61 - (0 - 4.52) = + 17.13 \text{ dB.} \quad (46)$$

Thus in this case an increase in gain greater than the free-space gain increase previously measured was observed. The second term in Equation 46 shows a difference in aperture-induced incremental aperture-to-medium coupling loss which is negative.

The intuitive rejection of a negative incremental coupling loss term on the basis it violates the premise of the maximum gain of an aperture being realized by plane wave illumination is not correct. Equations 6 and 8 are recopied here for convenience:

$$G_p = G_t + G_r - L_c \quad (6)$$

$$\Delta L_c = L_{c2} - L_{c1} = \Delta G_r - \Delta G_p \quad (8)$$

A negative incremental coupling loss will be observed for any comparison where L_{c1} is greater than L_{c2} .

A possible explanation of the form of the incremental aperture-to-medium coupling loss lies in consideration of the power patterns and "utilization" of the scattering media and common volume (12).

Remembering the scattering media was placed in the center of the range each time, the 316λ diameter transmitter and receiver would have comparable power patterns "on" the scattering media. The smaller apertures with their larger beamwidths would not have a signal in major portions of their effective power patterns. Consequently increasing the size of the receiving aperture, staying below the size of the transmitter, increases the portion of the receiving pattern being used. Thus along with the increased gain observed for plane wave illumination is found an increase in the efficiency of the aperture. This region is characterized by a negative difference in incremental aperture-to-medium coupling loss. In a similar manner, increasing the size of the receiving apertures above the size of the transmitter decreases the portion of the transmitted pattern which is "seen" by the receiving pattern. Thus the expected plane wave or free-space aperture gain increase is partially offset by the decreased efficiency of the transmitter. This region is characterized by a positive difference in incremental aperture-to-medium coupling loss.

The efficiency effects discussed here are simplified and accentuated by the physical restriction of the scattering media to a narrow region at the mid-point of the range. Such a restriction is not found in the tropospheric propagation paths of radio wave propagation in the atmosphere. Consequently the clarity and reproducibility of this effect is not seen in the results from tropospheric link measurements.

Though in sharp disagreement with published data the second trend of an aperture-to-medium coupling gain was as reproducible test after test as the first trend which agreed with published statements. In Yeh's collection (27) of 40 data points, nine points (22.5 percent)

showed an aperture-induced incremental aperture-to-medium coupling loss of exactly zero. Instantaneous measurements of received power showed up to 30 dB variations called fading, yet when mean signal levels were evaluated for two different antenna combinations and compared, 22.5 percent of the time the mean signal levels were exactly as calculated from free-space gain values. Two more points showed losses of 0.3 dB and 0.5 dB, but not one point was reported for a loss less than zero. Quite possibly whenever negative incremental aperture-to-medium coupling loss was observed the results were rounded off to zero. It seems to the author that considering the possibility that negative values of incremental coupling loss were not possible and exactly zero was correct, precise reporting would still have shown both positive and negative values about zero with the mean of those values tending to zero. Thus, the absence of points showing a negative incremental coupling loss is not considered conclusive evidence that such a negative loss cannot exist.

Chisholm, et al. (31), reported measurement of zero aperture-induced incremental aperture-to-medium coupling loss in their comparison of 412 MHz signals received by 60 and 28 foot antennas from a 60 foot transmitting antenna. They presented a plot of the distribution of the difference between the signals in dB for a typical month. That graph showed the difference to exceed 6.3 dB for 90% of the time, 7.0 dB for 50% and 8.0 dB for 10% of the time. For the antennas listed the calculated difference was 6.5 dB and so a report of -0.5 dB for the aperture-induced incremental aperture-to-medium coupling loss would seem to have been in order in place of the reported zero coupling loss. The

laboratory experiment found a -1.13 dB coupling loss for apertures in the ratios used by Chisholm, et al. This example is presented not as an indictment of the Chisholm, et al., paper but as an illustration demonstrating why the reported zero bound on aperture-induced incremental aperture-to-medium coupling loss may not be valid. In fact, their paper is to be commended for presenting a more complete set of data than most.

The study found no variation of aperture-induced incremental aperture-to-medium coupling loss with distance. Equation 38, recopied here for convenience, gives an expression which describes the composite results of the observed ΔL_c measurements.

$$\Delta L_{ci} = 18 \left| \log_{10} \frac{b_t}{b_i} \right| 2.50 \quad (38)$$

The only variable term included is the ratio of the diameters of the apertures. The roles of b_t and b_i obviously may be interchanged, once again showing the reciprocal nature of the effects of the transmitter and receiver. Though in sharp disagreement with published analyses, the independence of aperture-induced incremental aperture-to-medium coupling loss and distance was observed by Boithias and Battesti (22,30). Several physical limitations restricted their measurements to comparisons of combinations which varied distance only. They were unable to quantitatively compare combinations at each distance such as has been in Figure 5 through Figure 10. They did not differentiate between the two types of aperture-to-medium coupling loss as has been done for them here. They merely stated they found no variation of aperture-to-medium coupling loss as a function of distance. However a coupling loss term primarily determined by aperture gain as proposed by Boithias and Battisti from their other data and

compilation of selected results was not confirmed.

The results of test sequences already described considered the effect of changing only one aperture. These comparisons are the easiest to perform both in the lab and on the tropospheric links. The reported investigations purporting to evaluate aperture-to-medium coupling loss have employed only the aperture-change technique. The sector of coupling loss changes versus distance changes has not been attempted under that name in reported tropospheric propagation studies. Though requiring several steps, the laboratory apparatus allowed investigation of the decrease of power with increasing distance. The range power films were described previously in connection with their function of monitoring the alignment of the source beam centered on the transmitting aperture. The more important function of these measurements was to establish the reference level for the exact transmitted power for each range. The direct comparison of the range power films with the films recording the scattered power gave the variation of aperture-to-medium coupling loss as a function of distance.

Figure 11 is a plot of distance-induced incremental aperture-to-medium coupling loss. A direct comparison of Figure 11 with predicted values from the various theories was only of limited significance. The theories assumed several descriptions of the scattering media, none of which have been executed exactly in the laboratory experiment.

However holding the $h(\alpha)$ function fixed and varying the range (effectively varying the angular range θ) was the theoretical counterpart to the part of the evaluation shown in Figure 11. To the limited extent that both theory and experiment showed increasing ΔL_c for increasing

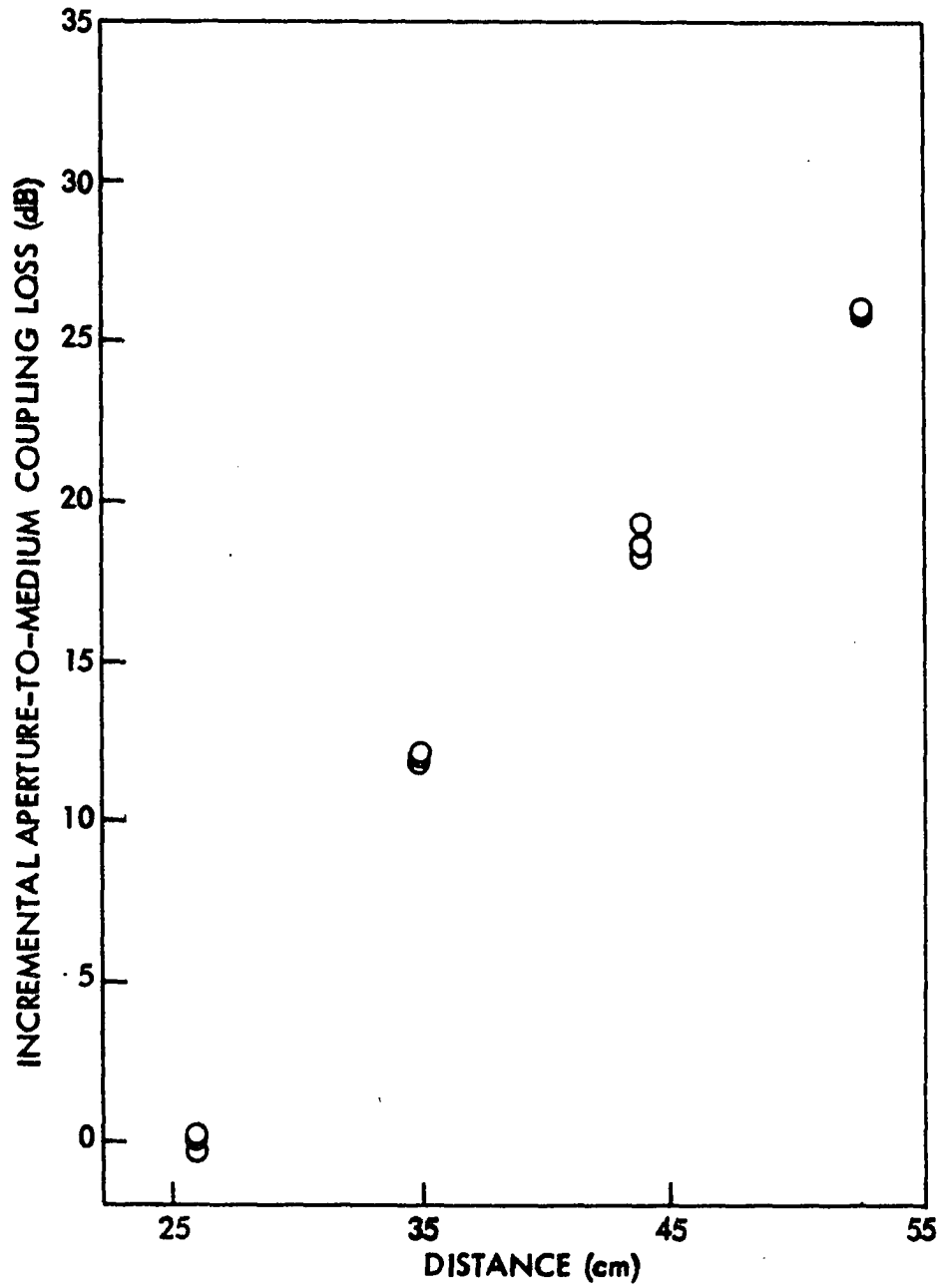


Figure 11. Distance-induced incremental aperture-to-medium coupling loss

distance, they agreed. The rate observed as ΔL_c experimental was much greater than the theories predicted.

Equation 8 recopied is

$$\Delta L_c = \Delta G_r - \Delta G_p \quad (8)$$

The comparison of two different G_p terms obtained by varying only the distance yielded

$$\Delta L_c = - \Delta G_p \quad (47)$$

Thus the path loss terminology of Chisholm, et al. (31) is equivalent to the distance-induced aperture-to-medium coupling loss description used here except for the additional quantity of the $1/d^2$ free-space power dependence which is an inherent part of Chisholm's results. Two studies reporting on path loss versus distance were Dinger, et al., (52) and Chisholm. Dinger described a study from about 25 to 725 miles on overwater paths which found a reasonably linear rate of path loss of 0.16 to 0.18 dB per nautical mile (0.086 to 0.097 dB per kilometer) at a frequency of 413 MHz. Chisholm gave the results of their overland studies at 412 MHz as showing a path loss rate which depended on distance. In the region of 180 to 350 miles they observed a path loss of 0.18 dB per mile (0.112 dB per kilometer). Drawing on the 1.16×10^6 length scale factor, the ranges used in the laboratory corresponded to 300, 400, 500, and 600 kilometers, and the laser light corresponded to 409 MHz radio waves. The results shown in Figure 11 have the line-of-sight distance dependence removed. Accepting the $1/d^2$ dependence discussed previously and adding it in to allow comparison with Dinger and Chisholm's results gives the values plotted in Figure 12. The laboratory points plotted are

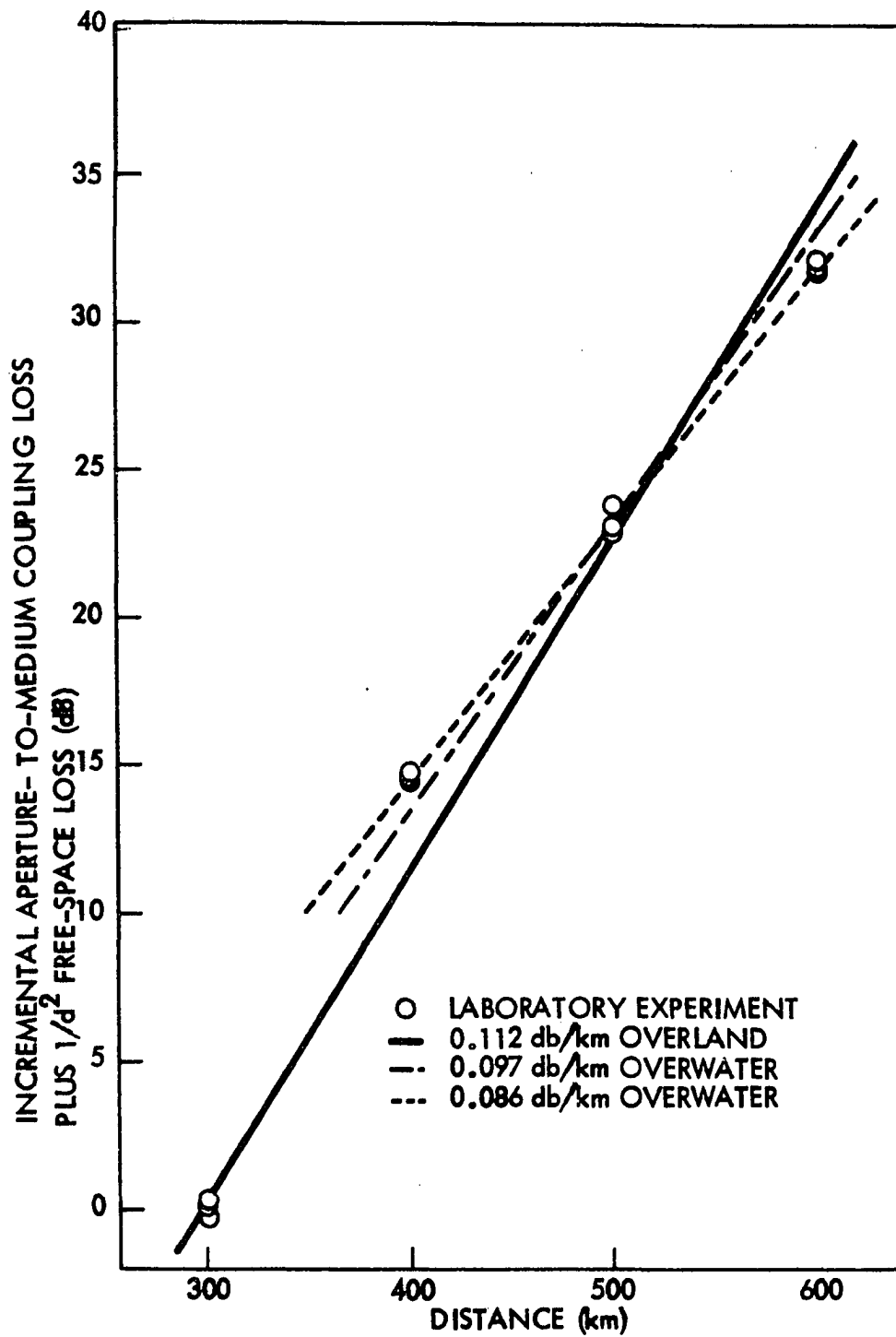


Figure 12. Laboratory and tropospheric link evaluation of distance-induced incremental coupling loss plus $1/d^2$ free-space power dependence

referenced to the shortest range of 300 km (or 26.0 cm actual). Again the inability to measure absolute losses in the laboratory limits the comparison to rates only. Consequently the overland and overwater distance attenuation rates shown in Figure 12 are arbitrarily positioned and only the relative rates merit consideration. Evaluation of the shortest to longest ranges roughly approximates Chisholm's two data points (300 to 600 km versus about 290 to 564 km) and shows 0.106 dB per km versus his reported 0.112 dB per km.

SUMMARY

Aperture-to-medium coupling loss is the term applied to the inability of large antennas to realize their full plane-wave gain when used in tropospheric radio wave propagation. Analytic investigation by several authors has resulted in widely divergent theories. Previous experimental results have not been successful in confirming or denying any of those theories or in solving the problem empirically as the experimentally determined values showed little correlation. Most of the experiments cited had been designed to study other aspects of tropospheric propagation and values of aperture-to-medium coupling loss measured and reported only when it directly affected the main results.

This paper described a system capable of investigating the question of aperture-to-medium coupling loss in the controlled environment of the laboratory. Though not precisely a model, strong use was made of a length scale factor of 1.16×10^6 and obvious similarities between the tropospheric propagation paths and the scatter propagation path developed for the setup. A helium-neon laser provided a high frequency, monochromatic, coherent source of high intensity. The propagation path was a narrow scattering media of spherical glass beads over a large, spherically-ground disc of glass. The transmitter and receiver were circular apertures. A photographic technique was developed to allow numerical evaluation of the power available at the receiver.

The particular physical limitations of the system restricted the results to evaluation of the change in received power versus the particular change in the configuration. It was not possible to measure total values

of aperture-to-medium coupling loss so the study's results are in the form of incremental coupling loss values. Changes in aperture sizes caused an aperture-induced incremental aperture-to-medium coupling loss which was independent of path length and was described by

$$\Delta L_c = 18 \left| \log_{10} \frac{\text{Diameter of transmitter}}{\text{Diameter of receiver}} \right|^{2.50}. \quad (48)$$

This independence of a distance term when investigating aperture changes is in disagreement with previous theories but has been previously observed by Boithias in his experiments. Changes in path distance showed a distance-induced incremental aperture-to-medium coupling loss of 0.092 dB per km when referred to an earth-sized range. Though known as path loss or range attenuation in some of the literature, it is included in the definition of aperture-to-medium coupling loss used in this paper. The combination of a distance term and an aperture-size terms into one variable, common to all the published theories, was not supported by this laboratory investigation.

Further work with the laboratory technique described is expected to include a variety of scattering medias, variation of scattering media position, increased range of aperture sizes, and possibly a complete change of scale by the use of other lasers.

LITERATURE CITED

1. W. J. Hartman and R. E. Wilkerson, "Path antenna gain in an exponential atmosphere," J. Res. NBS, vol. 63D, pp. 273-286, November-December, 1959.
2. K. A. Norton, "System loss in radio wave propagation," J. Res. NBS, vol. 63D, pp. 53-73, July-August 1959.
3. K. A. Norton, "System loss in radio wave propagation," Proc. IRE (Correspondence), vol. 47, pp. 1661-1662, September 1959.
4. W. J. Hartman, "Path antenna gain and comments on 'Properties of 400 MHz long distance tropospheric circuits'," Proc. IEEE (Correspondence), vol. 51, pp. 847-848, May 1963.
5. W. M. Gough, "Aperture-medium coupling loss in troposcatter propagation - an engineering appraisal," IEE, Conference Publication No. 48, pp. 93-100, 1968.
6. H. T. Friis, A. B. Crawford, and D. C. Hogg, "A reflection theory for propagation beyond the horizon," Bell Sys. Tech. J., vol. 36, pp. 627-644, May 1957.
7. H. Staras, "Further discussion of aperture-to-medium coupling loss," Proc. IEEE (Correspondence), vol. 52, pp. 100-101, January 1964.
8. K. Bullington, "Status of tropospheric extended range transmission," IRE Trans. Antennas and Propagation, vol. AP-7, pp. 439-440, October 1959.
9. F. DuCastel, Tropospheric radiowave propagation beyond the horizon. New York: Pergamon Press, 1966.
10. H. G. Booker and W. E. Gordon, "A theory of radio scattering in the troposphere," Proc. IRE, vol. 38, pp. 401-412, April 1950.
11. H. G. Booker and J. T. deBettencourt, "Theory of radio transmission by tropospheric scattering using very narrow beams," Proc. IRE, vol. 43, pp. 281-290, March 1955.
12. W. E. Gordon, "Radio scattering in the troposphere," Proc. IRE, vol. 43, pp. 23-28, January 1955.
13. H. Staras, "Forward scattering of radio waves by anisotropic turbulence," Proc. IRE, vol. 43, pp. 1374-1380, October 1955.

14. A. T. Waterman, Jr., "Some generalized scattering relationships in transhorizon propagation," Proc. IRE, vol. 46, pp. 1842-1848, November 1958.
15. K. Bullington, "Reflections from an exponential atmosphere," Bell Sys. Tech. J., vol. 42, pp. 2849-2867, November 1963.
16. C. M. Crain, "Survey of airborne microwave refractometer measurements," Proc. IRE, vol. 43, pp. 1405-1411, October 1955.
17. JTAC, "Radio transmission by ionospheric and tropospheric scatter," Proc. IRE, vol. 48, pp. 4-44, January 1960.
18. A. T. Waterman, Jr., "A rapid beam-swing experiment in transhorizon propagation," IRE Trans. Antennas and Propagation, vol. AP-6, pp. 338-340, October 1958.
19. E. E. Altshuler, U. H. W. Lammers, J. W. B. Day, and K. S. McCormich, "A troposcatter propagation experiment at 15.7 GHz over a 500 km path," Proc. IEEE (Letters), vol. 56, pp. 1729-1731, October 1968.
20. H. Staras, "Antenna-to-medium coupling loss," IRE Trans. Antennas and Propagation, vol. AP-5, pp. 228-231, April 1957.
21. N. A. Armand and B. A. Vvedenskii, "On the loss of gain mechanism with narrow-beam antennas in long distance ultra-short-wave tropospheric propagation," Radiotechnic and Electronics, vol. 4, pp. 1594-1601, 1959.
22. L. Boithias, "An experimental study of antenna gain loss," IEEE Trans. Antennas and Propagation (Communications), vol. AP-15, pp. 578-579, July 1967.
23. F. W. Schott, "On the response of a directive antenna to incoherent radiation," Proc. IRE, vol. 39, pp. 677-680, June 1951.
24. L. P. Yeh, "Experimental aperture medium coupling loss," Proc. IRE (Correspondence), vol. 50, p. 205, February 1962.
25. D. C. Hogg, "The aperture-to-medium coupling loss in beyond-horizon propagation," Proc. IRE (Correspondence), vol. 50, pp. 1929-1530, June 1962.
26. A. B. Crawford, D. C. Hogg, and W. H. Kummer, "Studies in tropospheric propagation beyond the horizon," Bell Sys. Tech. J., vol. 38, pp. 1067-1178, September 1959.
27. L. P. Yeh, "Experimental aperture-to-medium coupling loss," IEEE Trans. Antennas and Propagation (Communications), vol. AP-14, pp. 663-664, September 1966.

28. J. L. Levatich, "Antenna gain-loss estimates," Proc. IRE (Correspondence), vol. 50, pp. 2137-2138, October 1962.
29. C. A. Parry, "The aperture-to-medium coupling loss in tropospheric scatter systems," Proc. IEEE (Correspondence), vol. 51, pp. 933-934, June 1963.
30. L. Boithias and J. Battesti, "Etude experimentale de la baisse de gain d'antenne dans les liaisons transhorizon," Annals des Telecommunications, pp. 221-229, September-October 1964.
31. J. H. Chisholm, W. E. Morrow, Jr., B. E. Nichols, J. F. Roche, and A. E. Teachman, "Properties of 400 MHz long-distance tropospheric circuits," Proc. IRE, vol. 50, pp. 2464-2482, December 1962.
32. J. H. Vogelmann, J. L. Ryerson, and M. H. Bickelhaupt, "Tropospheric scatter system using angle diversity," Proc. IRE, vol. 47, pp. 688-696, May 1959.
33. J. H. Chisholm, P. A. Portman, J. T. deBettencourt, and J. F. Roche, "Investigations of angular scattering and multipath properties of tropospheric propagation of short radio waves beyond the horizon," Proc. IRE, vol. 43, pp. 1317-1335, October 1955.
34. K. Bullington, W. J. Inkster, and A. L. Durke, "Results of propagation tests at 505 MHz and 4090 MHz on beyond-horizon paths," Proc. IRE, Vol. 43, pp. 1306-1316, October 1955.
35. E. Dyke, "Boithias' and other papers on antenna coupling loss," IEEE Trans. Antennas and Propagation (Communications), vol. AP-14, pp. 665-667, September 1966.
36. A. M. J. Mitchell and T. K. Fitzsimons, "Experiences in tropospheric scatter propagation experiments," IEEE Trans. Antennas and Propagation (Communications), vol. AP-17, May 1969.
37. M. I. Skolnik, "A method of modeling array antennas," IEEE Trans. Antennas and Propagation (Communications), vol. AP-11, pp. 97-98, January 1963.
38. W. H. Huntley, "A new approach to antenna scaling," IEEE Trans. Antennas and Propagation (Communications), vol. AP-11, pp. 591-592, September 1963.
39. D. T. Gjessing and F. Irgens, "Scattering of radio waves by a moving atmospheric rippled layer: a simple model-experiment," IEEE Trans. Antennas and Propagation, vol. AP-12, pp. 703-709, November 1964.
40. M. R. Guidry, "A model of terrestrial radio wave propagation using a laser," Unpublished Ph.D. thesis, Ames, Iowa, Library, Iowa State University of Science and Technology, 1965.

41. R. E. Post, M. R. Guidry, and D. F. Rost, "A laboratory model for studying transhorizon radio wave propagation phenomena," *Radio Science*, vol. 3, pp. 523-527, June 1968.
42. R. E. Post and D. F. Rost, "Laboratory model studies of transhorizon radio wave propagation phenomena," *IEE, Conference Publication No. 48*, pp. 77-84, 1968.
43. A. T. Waterman, Jr., N. H. Bryant, and R. E. Miller, "Some observations of antenna-beam distortion in transhorizon propagation," *IRE Trans. Antennas and Propagation*, vol. AP-5, pp. 260-266, July 1957.
44. A. T. Waterman, Jr., "A rapid beam-swinging experiment in transhorizon propagation," *IRE Trans. Antennas and Propagation*, vol. AP-5, pp. 338-340, October 1958.
45. D. F. Rost, "Model studies of transhorizon radio wave propagation phenomenon," Unpublished M.S. thesis, Ames, Iowa, Library, Iowa State University of Science and Technology, 1967.
46. R. E. Post and D. F. Rost, "Modeling UHF transhorizon scatter propagation," *IEEE Trans. Antennas and Propagation (Communications)*, vol. AP-16, pp. 612-613, September 1968.
47. L. G. Trolese, "Characteristics of tropospheric scattered fields," *Proc. IRE*, vol. 43, pp. 1300-1305, October 1955.
48. G. F. Koch and K. S. Kölbig, "The transmission coefficient of elliptical and rectangular apertures for electromagnetic waves," *IEEE Trans. Antennas and Propagation*, vol. AP-16, pp. 78-83, January 1968.
49. P. Glafkides, Photographic Chemistry. London, England: Fountain Press, 1958, vol. 1, pp. 200-245.
50. J. W. Goodman, Introduction to Fourier Optics. San Francisco, Calif.: McGraw-Hill, 1968, pp. 63-65.
51. S. Silver, Microwave Antenna Theory and Design. Lexington, Mass.: Boston Technical Lithographers, Inc., 1963, p. 177.
52. H. E. Dinger, W. E. Garner, D. H. Hamilton, and A. E. Teachman, "Investigation of long-distance overwater tropospheric propagation at 400 MHz," *Proc. IRE*, vol. 46, pp. 1401-1410, July 1958.

ACKNOWLEDGEMENTS

The work described was sponsored by the Engineering Research Institute at Iowa State University. The author wishes to thank his major professor and project director Dr. R. E. Post for his assistance and encouragement. The recording microphotometer used for all film reductions belonged to the Ames Laboratory of the U.S. Atomic Energy Commission and was assigned to Dr. W. L. Sutherland. Without Dr. Sutherland's continued cooperation this project would not have been possible.

The author would especially like to thank his wife and family for their patience and support.